BELLCOMM, INC.
955 L'ENFANT PLAZA NORTH, S.W. WASHINGTON, D. C. 20024

B70 02023

SUBJECT: Photography of Ground Sites from AAP Orbit - Case 610

DATE: February 12, 1970

FROM: D. A. De Graaf
E. W. Radany

ABSTRACT

Opportunities to photograph ground targets from the AAP orbit were analyzed for S190, the Multispectral Photographic Facility:

1. Solar lighting conditions alternate from good to bad on a 60-day cycle. Care must be taken to ensure that good lighting coincides with the first AAP mission of 28 days.

2. At U.S. latitudes good lighting conditions are abundant in summer, but vanishingly few in winter.

3. The probability of being able to photograph a particular ground site peaks sharply if its latitude is at or near the 50° orbit inclination.

It has been the plan to do S101, the predecessor to S190, with the Workshop maneuvered to a local vertical attitude. That is, the cameras will be mounted rigidly against a window and the entire cluster turned to look straight down. We have analyzed the alternate strategy of maintaining the standard solar-inertial attitude and deflecting the camera to acquire the ground site through the window.

1. The number of photographic opportunities for a specific ground site is almost as great if a line-of-sight angle of incidence (to the window) up to 50° is permitted.

2. Substantial advantages are realized in the areas of attitude control, electrical power, thermal control, efficient utilization of astronauts, and compatibility with other Workshop activities.

3. A larger, and possibly thicker, window would be needed to provide an unobstructed view and to avoid optical distortion.

BELLCOMM, INC.
955 L'ENFANT PLAZA NORTH, S.W. WASHINGTON, D. C. 20024

B70 02023

SUBJECT: Photography of Ground Sites from AAP Orbit - Case 610

DATE: February 12, 1970

FROM: D. A. De Graaf
E. W. Radany

MEMORANDUM FOR FILE

1.0 Introduction

Experiment S101, Multispectral Photography, has recently been replaced by S190, the Multispectral Photographic Facility, on AAP. By whatever name, this equipment will be operated on all three missions in Saturn Workshop I. Its integration has been a problem ever since the decision for the dry Workshop was made, mainly because this experiment must be pointed toward the earth. With the old wet Workshop, the ATM was not along on two of the three missions and a capacious Workshop Attitude Control System (WACS) was available for attitude maneuvers. Accordingly, it was planned to mount the S101 cameras rigidly against a window and maneuver the entire Workshop to the local vertical attitude to aim the cameras. With the dry Workshop, the ATM is with us full time so that departures from the solar-inertial attitude will interfere with its operation. The ATM appears to have thermal problems when it is not properly pointed at the sun that curtail the allowable duration of local vertical operation. Finally, the WACS is replaced by Control Moment Gyros (CMG) and a cold-gas Thruster Attitude Control System (TACS). The CMG's evidently have insufficient muscle to perform maneuvers out of the solar-inertial attitude and use of the cold-gas system is relatively expensive, weight-wise. Nevertheless, alternative schemes have not been widely discussed and it is still planned to operate the multispectral cameras in the local vertical attitude.

This memo explores the possibility of remaining in the solar-inertial attitude during the ground photography. We presume the existence of an adequate window in the MDA (or elsewhere) on the side away from the ATM so that the center of its field of view is always directly along the sun's rays. This gives a favorable geometry because the field of view includes potential targets that are well lit by the sun. Targets outside this field of view are not well lit and could not be photographed anyway.

The main part of this memo deals with the orbit geometry and calculation of viewing opportunities. Other topics discussed are optical distortions due to the window that must be guarded against and improvements in operational procedures that would accrue from this alternate method.

2.0 Description of the Experiment

The S190 facility uses a ganged array of six cameras to simultaneously photograph the ground in different portions of the visible and infrared spectrum. The films will be returned to earth and analyzed for clues to agricultural and geological conditions. Comparison pictures will be taken of the same areas from high flying airplanes. It is also important to include in the photographs "ground truth sites" where the condition of vegetation and geology are accurately known from ground surveys. The intent is to determine how much information can be reliably deduced from space photographs in comparison to the photographs from the aircraft and from ground measurements. Specific ground truth sites are not yet designated, but we understand there will be many, perhaps 100, sprinkled throughout the U.S.

Generally, the camera shutters will be triggered by an intervalometer to obtain a swath of overlapping pictures. It may be set for 60% overlap if stereo analysis is desired, or 10% overlap otherwise. Detailed requirements have not yet been stated concerning how many ground truth sites should be included in a swath, or how long a swath should be. Therefore, we will consider only the problem of photographing a single point target.

Two important constraints are imposed to assure high quality photos. The view must be nearly straight down along the local vertical, and the site must be well lit by the sun. The first requirement minimizes dimensional distortion and facilitates comparisons with maps of the area. The Hasselblad cameras, specified in the S101 experiment, use 70 mm film and have 150 mm, f/2.8 lenses. The picture area is 55 mm square which gives a $\pm 10.5°$ field of view. From 235 nm altitude each picture covers an area 86 nm square. If the camera center line is arbitrarily tied exactly to the local vertical, a prospective target must pass within this rather tiny area. As will be shown later, the odds on this happening are very slim. More frequent opportunities are obtained if the target line-of-sight is allowed to make a larger angle with the local vertical. We understand the Principal Investigator is inclined to permit angles up to about 20°. The camera itself need be deflected from the nadir only enough to bring the target into the picture.

Good lighting is defined to exist when the sun is no more than 60° from the vertical at the site. In the wintertime this is rather rare, so the standards are lowered; a 70° sun angle is okay.

3.0 Ground Site Visibility

3.1 Description of Geometry

The dynamic and geometric relations that determine when the nadir angle and sun angle constraints are satisfied are difficult to visualize, and are further complicated when an inertially oriented viewing window is interjected into the system. We have resorted to the computer to find specific instances that satisfy all the constraints. However, the principles can be discussed with the aid of Figure 1. (Greater detail is presented in the Appendix.)

The spherical geometry is unwrapped and the orbit's ground track is plotted in latitude-longitude coordinates. Since the orbit inclination is 50°, the peak latitude is also 50°. The horizontal axis represents longitude measured from the orbit's ascending node, rather than the usual earth-fixed Greenwich meridian. The earth rotates eastward in this coordinate system, one rotation per nodal day. The coordinates are not quite inertially fixed, however, because torque from the earth's oblate gravity field precesses the orbit plane, causing the ascending node to shift slowly westward. The equation listed in the Appendix yields a regression rate of 5.068128° per 24 hours for the AAP orbit. Therefore, a point on the earth rotates node to node in slightly less than 24 hours, 23.602225 hours to be exact.

For a ground site to be photographed, it must move into the plane of the orbit at one of two points: the ascending or the descending intersection of the orbit ground track with the latitude circle, as illustrated for a 40° site. Earth's rotation will bring the ground site through each point once each day.

Thus, we have two moving points in Figure 1: the ground site, which makes one rotation along its latitude circle each day (a nodal day, that is, of 23.602225 hours), and the satellite ground track, which traverses the orbit path in approximately 90 min. Photography requires that these points pass within a small distance of each other, which is determined by the maximum permissible angle between the line-of-sight and the local vertical. In the computer runs which search out such opportunities, this nadir angle was treated parametrically; values of 10°, 20°, and 30° were used.

The computer program takes advantage of the fact that the ground site's motion is exactly repetitive each nodal day, and the orbit ground track remains constant in the rotating coordinates of Figure 1. Only the satellite's phase angle varies from day to day. The exact orbit period depends primarily on altitude, and one must be careful to calculate nodal period, instead of the usual perigee period, with due allowance for nodal regression as indicated in the Appendix. At 235 nm altitude, it works out to 93.196399 min, so that in one nodal day the satellite completes 15.195152 orbits. The fractional part of this number gives rise to a new initial phase angle each nodal day. The pattern of this change is non-repetitive and appears substantially random. At other altitudes, it is theoretically possible to get a repetitive pattern that would upset the viewing probabilities, but this is very unlikely.

The sun's position in our nodal coordinate system moves slowly eastward, due mainly to the nodal regression but augmented by the annual rotation of the earth-sun line in inertial space. It takes 60.304152 nodal days to make a full circuit. The sun's latitude, or declination, also oscillates with the seasons between +23.5° and -23.5°. This is the longest period variation encountered in this problem and one of the most important.

The lighting requirement can also be visualized with the aid of Figure 1. At the subsolar point the sun's rays are incident vertically; the angle of incidence increases with distance from this point. Good lighting exists within a circular region centered at this point with a radius of 60° of earth central angle. The 60° circle of good lighting is shown in Figure 1 at two nodal longitudes with the sun at the +23.5° extreme northerly declination. (The distortion in mapping the circle into these coordinates is evident.) At the first position it is apparent that the photographic intersections will remain continuously dark for many days. With time, the region slides eastward to the second position. The photographic intersections then will remain continuously well lit for the remainder of the 60-day cycle. For high latitude sites the duration of good lighting is far longer in summer than in winter. Indeed, at the winter solstice, sites higher than 36.5° never receive good lighting at any time in the 60-day cycle.

Optimum lighting occurs when the sun happens to be at the same nodal longitude as the photographic intersection. Optimum lighting at the ascending intersection

precedes that at the descending intersection by a number of days that depends on the site latitude. They tend to merge as the latitude approaches the inclination.

Application of the third and final constraint is more difficult to describe. It requires that the line-of-sight to the ground site make an angle of incidence with the window of no more than 50°, for example. This admits a conical field of view centered along the sun's rays, because of the vehicle's solar inertial orientation. During an encounter the line-of-sight slews rapidly as the satellite passes by. While the line-of-sight is moving within the acceptable conical region around the nadir direction, the window angle may change between acceptable and unacceptable. The computer program allows only encounters that at some time simultaneously satisfy both conditions; the duration of time for which both conditions were simultaneously satisfied was not calculated, however.

3.2 Computed Results

The computed photographic opportunities are shown in Figures 2 through 8. The first three charts show opportunities and sun angle versus day of the year for representative U.S. sites at 32°, 40° and 48° latitude. Tick marks above and below the time scale denote daily photo opportunities throughout the year at the ascending and descending intersections, respectively, which satisfy the 20° nadir angle, 60° solar lighting angle, and 50° window angle of incidence constraints. The solar angles from vertical at each intersection are also plotted. The 60-day cyclic variation in solar angle controls the photography, with clusters of opportunities occurring whenever the sun angle drops below 60°. The annual seasonal variation in solar declination also has a substantial effect. Because the computation was started with the sun at the vernal equinox, the maximum northerly solar declination occurs at about 90 days and the maximum southerly declination at 270 days. In the winter, even the best sun angle is not good enough for the 48° site and only briefly good enough for the 32° site. Summertime provides excellent coverage; the period of continuous good lighting at one or both of the 40° intersections, for instance, lasts up to 37 days.

Initial conditions in the computer run for the positions of satellite, ground site, and sun were arbitrarily selected, with no attempt to duplicate the conditions that would be established by the launch of AAP-1. Thus, the

time scale on these figures should not be interpreted as time into the AAP mission. The simplest possible initial conditions were used: at the beginning of day 0 in our nodal coordinate system, (latitude, nodal longitude), the satellite was at (0,0), the ground site at (ϕ,0), and the sun at (0,0). Thus, the sun started from the vernal equinox and coincided with the ascending node of the orbit. From these initial conditions one can easily interpret the effects of the 60-day rotation of the sun-node angle and the annual oscillation of the sun's declination. The initial position of the satellite in its orbit and of the ground site on its latitude circle determine the specific occurrences of opportunities throughout the year, but since these results appear substantially random, different initial conditions would alter the specific instances but not the general pattern or total number of opportunities.

While the initial values were picked for simplicity, it happens, fortuitously, that the AAP orbit will be not too different, with respect to the initial sun position which has such a crucial effect on lighting. The planned springtime launch will ensure a northerly declination during most of the eight months. The planned late afternoon launch is also good because it establishes a favorable starting point for the orbit node relative to the sun. A 3 p.m. launch, for example, places the ascending node only 12° east of the sun, ensuring that the first period of good lighting in the northern hemisphere will begin promptly and last through most of the 28-day mission. The pattern of lighting variation revealed in the data shows blackout periods long enough to contain an entire 28-day mission. A less favorable launch time of day than is currently planned could preclude S190 photography from the AAP-2 mission. The 56-day missions are no problem, since the good lighting recurs every 60 days, and photographic opportunities are bound to occur sometime during the mission, no matter what the initial sun position may be.

Figure 5 compares good lighting windows and photo opportunities through the year for 11 sites at different latitudes (not equally spaced). Sites above 32° (really 36.5°) are out of luck for wintertime photography. However, in the summertime when lighting is good the opportunities are densely spaced for these northern sites. Going toward the equator, the opportunities become spread more uniformly and the ascending and descending intersection lighting periods overlap less.

In Figures 6, 7, 8 and 9 the cumulative annual photo opportunities of a site at the specified latitude are plotted versus the site latitude. The effects of varying the limits on window angle, nadir angle, and sun angle are shown here as parametric curves. Reference values of these angles of 50°, 20° and 60°, respectively, were used as a base of comparison. Figure 6 shows the results when the limit on line-of-sight angle of incidence on the window is changed from 50° to 40° or 180°. An angle limit of 180° is in fact no limit at all; it corresponds to an omni-directional window and is a trick to eliminate the window angle constraint from the problem. This curve can properly be interpreted as photo opportunities that would be available if the Workshop flew in the local vertical attitude, since in that case, the window would always be pointed correctly and would exclude no opportunities. However, these results are calculated for a nadir angle up to 20°, and since the camera field of view is only 10° we are presuming the camera can be deflected from straight down when necessary to acquire the target. This is simple in the solar inertial mode, since the camera orientation has to be adjustable anyway, but it may not be realistic for the local vertical mode with the camera mounted rigidly against the window. Nevertheless, we see the effect of having the window oriented solar inertially, by itself, is not very severe if window angles up to about 50° are permitted.

Figure 7 shows the effect of limiting the angle between the line-of-sight and the local vertical to 10°, 20° and 30°. The number of opportunities is approximately proportional to the radius of this field of view.

In Figure 8, we see the slight increase obtained by changing the sun angle limit from 60° to 70° from the vertical.

Figure 9 shows annual photo opportunities from the local vertical mode, assuming the cameras are pointed straight down so the nadir angle is limited to the camera's 10° half angle. This restriction results in the fewest photo opportunities of all!

In all these cases, the variation with latitude in the number of photographic opportunities is impressive. Sites at a latitude equal to the inclination of 50° have about four times as many photo opportunities as sites below 35°. This is due to the unequal probability of satellite dwell time in each latitude band. The satellite spends a disproportionate time at or near 50°. Note that this effect

is so powerful that more opportunities occur at 50° even though the annual duration of good lighting at high latitudes is much less than at lower latitudes.

The shaded area in Figure 6 represents the geographical extent of the U.S. At each latitude the height is a relative measure of the east-west width of the country, that is, the longitudinal extent scaled by the cosine of the latitude. This gives an idea of the potential distribution of photographic targets. It is evident that the selection of 50° for the orbit inclination has put the easiest sites for photography just into Canada.

3.3 β Angle Limit

In connection with the current plans to maneuver the Workshop to the local vertical attitude there has been recurrent discussion of limiting such maneuvers to times when the β angle is less than 30°. This would be a most unfortunate constraint, as it would eliminate a good many otherwise acceptable photographic opportunities. β is the angle between the solar vector and the orbit plane and may be visualized on Figure 1 as the perpendicular distance from the sun's position to the orbit ground track. As the sun slowly moves eastward, β oscillates between positive (northerly) and negative (southerly) values. The best lighting occurs when the sun's position is due south of the photographic intersection and this invariably entails a negative value of β. The largest negative values of β occur when the sun is midway between the ascending and descending photographic intersections.

The disastrous effects of such a constraint are shown in Figure 10. At the bottom are the good lighting windows with specific photographic opportunities calculated for the local vertical mode (60° sun angle, 10° nadir angle, no window constraint). The variation of β is also plotted. In the summer when the sun is well north of the equator, β remains above -30° and in the winter not much photography can be done anyway because of the poor lighting. But in the spring and fall, major portions of the good lighting periods would be eliminated by a 30° limit on β.

4.0 Optical Effects of a Window

Refraction of the light rays passing through the Workshop window can degrade the optical system more when the camera is tilted than when it is parallel to the window normal. For a window that is truly flat, homogeneous, and with parallel surfaces, Snell's Law shows that every ray that enters the window leaves along an exactly parallel path - the refractions at front and rear surfaces are equal

and opposite. However, the Workshop atmosphere pressure will bulge the window outward and this will no longer be true. Deformation analysis for a uniformly loaded circular plate with a clamped edge shows the displacement will be of the form

$$y = \frac{K(a^2-r^2)^2}{t^3} \tag{1}$$

where a is the window radius, r is the radial distance from the center, t is the thickness and K is a constant which depends on the mechanical properties of the glass and the pressure is about 0.87×10^{-7} for silica glass and a 5 psi internal pressure. A cross section of the bulging window and a typical refracted ray are shown in Figure 11. (The actual Workshop window will almost certainly be rectangular, not circular. However, assuming a circular window simplifies the calculations to estimate the magnitude of the optical distortion and is conservative).

Figure 12 is an enlarged view of a ray penetrating the outer surface at radial distance r_A, and emerging at r_B. θ_1, θ_2, θ_3, and θ_4 are ray angles measured with respect to the local surface normals at the points of penetration, so they are related by Snell's Law:

$$\begin{aligned} n \sin\theta_1 &= n' \sin\theta_2 \\ n' \sin\theta_3 &= n \sin\theta_4 \quad , \end{aligned} \tag{2}$$

where n is the index of refraction of space, and n' is the index of refraction of the glass. Because of the bulge, the normals to the surface will be tilted slightly by the angles γ_A and γ_B relative to the principal axis of the window. The ray directions measured relative to the principal axis on each side of each interface are related by:

$$\begin{aligned} \phi_1 &= \theta_1 - \gamma_A \\ \phi_2 &= \theta_2 - \gamma_A \\ \phi_3 &= \theta_3 - \gamma_B \\ \phi_4 &= \theta_4 - \gamma_B \end{aligned} \tag{3}$$

where $\phi_2 = \phi_3$, since the interior ray travels in a straight line. Combining these equations we obtain

$$\phi_4 = \sin^{-1}\left\{\frac{n'}{n}\sin\left[\sin^{-1}\left(\frac{n}{n'}\sin(\phi_1+\gamma_A)\right) + (\gamma_B-\gamma_A)\right]\right\} - \gamma_B \quad (4)$$

It is easily verified that $\phi_4 = \phi_1$ if $\gamma_A = \gamma_B = 0$ (no window bulge). Small angle approximations can be used to simplify this equation since γ_A and γ_B are always very tiny angles:

$$\phi_4 - \phi_1 \approx \left(\frac{n'}{n}\frac{\cos\phi_2}{\cos\phi_4} - 1\right)\left(\gamma_B - \gamma_A\right) \quad (5)$$

The tilt of the surface is obtained from (1), observing that

$$\gamma = \tan^{-1}\frac{dy}{dr} \approx \frac{dy}{dr} \quad (6)$$

To first order the back surface has exactly the same contour as the front surface, so the angle of tilt depends only on r, the distance from the center.

$$\gamma_B - \gamma_A \approx \frac{d\gamma}{dr}(r_B - r_A) = \frac{d\gamma}{dr}\, t\, \tan\phi_2 \quad (7)$$

The ray's change in direction, $\phi_4 - \phi_1$, will cause an apparent lateral displacement in the position of the object which, at a range R of 235 nm, is

$$D = R(\phi_4 - \phi_1) \quad (8)$$

Combining Equations (1), (5), (6), (7) and (8), we obtain

$$D = R\left(\frac{n}{n'}\frac{\cos\phi_4}{\cos\phi_2} - 1\right)\frac{4K}{t^2}\left(a^2 - 3r^2\right)\tan\phi_4 \qquad (9)$$

This displacement is plotted in Figure 13 against radius of penetration for angles of incidence of 10°, 30° and 50° for a window of 15" radius, 1/2" thickness, and an index of refraction of 1.5. The effect increases sharply with angle of incidence.

The variation of displacement across the window smears the image and degrades the resolution of the camera system. Light rays from a single point on the earth's surface are substantially parallel when they arrive at the Workshop but are refracted differently at different positions across the window. For the rays that actually enter the camera lens, the apparent source will vary so that a sharp focus will not be obtained. The image will be smeared over a distance corresponding to the differential object displacement experienced by light rays over the width of the camera lens. The worst smearing occurs if the camera is near the edge of the window where the differential displacement is the greatest. Smearing is less for a thicker window because it is stiffer. Figure 14 shows the differential object displacement between the limiting rays from a point object that enter a camera for lens diameters from 1 to 4 inches. (A diameter of 2" may be regarded as typical; with the 150 mm focal length lens, it corresponds to an F stop of 3.)

Ideally, this smear should not be allowed to exceed the resolution distance that is inherent in the rest of the camera system which has been quoted as 30 meters. A window thickness of about 0.7 inches is called for. This is substantially thicker than is needed simply to withstand the pressurization stress safely.

Differential refraction will also distort the field of view of each camera differently so that the scale factor between position in the object field and image position on the film will be slightly different for each camera. In projecting the multispectral pictures it will be impossible to make all four images exactly overlay one another over the full area of the picture. Figures 14, 15 and 16 show the camera geometry and ray pattern for a maximum camera deflection of 40° around the short axis of

symmetry. For each ray the apparent shift in object position was calculated for a .73" thick window and plotted in Figure 17. We see the maximum displacement for any object in the field of view is only slightly more than the 30 meter resolution distance. Slight adjustment of the projector boresight would even improve this excellent registration. It is safe to conclude the registration will not be a problem if the window is thick enough to satisfy the resolution criterion.

5.0 Implementation Hardware

5.1 Camera Mount

A two axis camera mount is required to aim the cameras along the local vertical from the solar inertial attitude. In this attitude the long axis (X axis) of the Workshop is in the orbit plane and perpendicular to the sun vector. The ATM side (or -Z axis) is rolled out of the orbit plane by the β angle to face the sun. If one axis of the camera mount provides rotation about the X axis it can compensate for the β angle roll. The second axis then would swing the camera in the orbit plane. At orbital noon the local vertical is perpendicular to the vehicle X axis; earlier or later the local vertical is at some angle to this direction.

The axes of rotation must be calibrated so the astronaut can preset these angles and activate the shutter intervalometer as commanded by the ground controllers.

Long swaths of continuous overlapping pictures cannot be easily made from the solar inertial attitude because the local vertical direction appears to rotate at 4 deg/min relative to the window and would move completely across the camera's field of view in 5 minutes. In this time the satellite covers a distance of 1200 miles and takes 15 pictures.

In the local vertical mode, camera operation can continue as long as there is interesting, well lighted terrain beneath the satellite. However, it is not clear how extremely long continuous swaths of pictures will benefit the stated objectives of the experiment. Indeed, it would seem preferable to expose the film more selectively to enhance the coverage of ground truth sites and to avoid photography of solid cloud cover. The experiment objectives require the exposure of 800 frame sets during the three AAP missions. The capacity of the attitude control system is believed to permit use of the local vertical mode only 45 times for one orbit each. It would be necessary, therefore,

to expose 18 frame sets on each pass, covering a 1400 mile swath. The solar inertial mode would permit a more selective and frequent use of the cameras.

5.2 Window Size

To deflect the camera rack by a substantial angle, a larger window would be required to avoid occluding the view at the edge. Figures 17 and 18 give a general idea of the situation. The six camera center lines are mounted in a 2 x 3 rectangular array that is 11.5 x 14 inches as shown in Figure 17. The elliptical areas of the ray intersections with the window are shown in Figure 18 for 40° tilts about the long axis, the short axis, and the diagonal of the camera rack. All the light rays pass within a 27.4" x 25.8" rectangular area, so the window would have to be at least that big. For this graphical construction, the camera rack moved about a center of rotation 2" outside the window; this was found to give very nearly the optimum penetration pattern.

6.0 Timeline Considerations

Because it is so difficult for the attitude control system to make the transition between solar inertial and local vertical attitudes, it will probably be necessary to enter the local vertical mode at orbital midnight, remain one or two full orbits, and resume solar inertial again at orbital midnight. Astronaut participation will be required for 1-1/2 hours or more; other activities, notably the ATM experiments, will have to be suspended. The actual picture taking lasts only about 11 minutes and can easily be accomplished by one astronaut.

This inefficiency would be mitigated if other earth resource experiments were to be done and if their objectives and operating constraints dictated concurrent operation with the photography. However, if S190 must be done alone, it would be far easier in the solar-inertial mode.

7.0 Conclusions

The relative motion of satellite, ground site, and orbit plane relative to the sun impose some important patterns on the availability of photographic opportunities, regardless of the Workshop's attitude:

1. Good lighting recurs on a 60-day cycle due to the westward regression of the orbit plane relative to the sun.

2. The duration of good lighting is greater in the summer - about 37 days at 40° latitude but is virtually nonexistent in the winter for most U.S. points.

3. A given ground site passes under the orbit plane twice each day, on the ascending and descending halves of the orbit. Whether the satellite simultaneously passes overhead is a matter of chance. The probability is proportional to the allowable angle between line-of-sight and local vertical and is pretty low. A large area target like the U.S. can be photographed every day during the period of good lighting when it rotates under the orbit, if one is not particular about the place being photographed.

4. Sites at or near a latitude equal to the 50° orbit inclination have many more chances to be photographed during a year than those below 45°. This occurs despite the bad lighting conditions in the winter.

Considering the relative merits of solar inertial versus local vertical attitude for this experiment, we observe:

1. Nearly as many photographic opportunities occur in the solar-inertial mode if the window line-of-sight angle of incidence is allowed to be as big as 50°. Considering that it would be easy to deflect the cameras up to 10° from straight down in the solar-inertial mode, while this may be impossible in the local vertical mode, we actually find more chances to photograph a specific site from the solar-inertial mode than from the local vertical mode.

2. Remaining in the solar-inertial mode would eliminate the need for expending attitude control propellant, eliminate potential problems in electrical power generation and thermal control, avoid disruption of other Workshop activities, and permit a single astronaut to operate the equipment in the least amount of time.

3. Solar-inertial operation does not limit the number of times the equipment may be operated, so greater selectivity can be exercised, and the effects of cloud cover minimized.

4. To do the experiment effectively from the solar-inertial attitude requires:

   a. A redesigned window, larger and thicker.

   b. A two-axis calibrated camera mount.

8.0 Acknowledgment

The authors gratefully acknowledge Miss L. K. Hawkins' programming assistance in this study.

D. A. De Graaf

E. W. Radany

1025-$\frac{DAD}{EWR}$-li

Attachments

APPENDIX

Orbital Plane Geometry

The geometry of the orbit groundtrack and a typical ground site latitude (ϕ_G) is shown in Figure A. The true anomaly of the satellite, η, increases linearly with time and can be used conveniently as the independent variable for motion in place of time. However, since the orbit is circular, it cannot be measured meaningfully from perigee and must be measured from the ascending node. When the satellite is at a true anomaly η, latitude and nodal longitude can be obtained from the spherical trig relations:

$$\sin \phi = \sin \eta \sin i$$

$$\tan \lambda = \tan \eta \cos i$$

If the line-of-sight to a target is constrained to be within P degrees of the nadir, there is a circular field of view of radius ρ measured as an earth central angle

$$\rho \simeq \frac{h}{R_e} P = \frac{235.}{3440.} P,$$

where h = orbit altitude and R_e = radius of the earth. Whenever the satellite's latitude is within the band $\phi_G \pm \rho$, some portion of the ϕ_G latitude circle will be visible. The visible segment will extend from $\lambda-\Delta\lambda$ to $\lambda+\Delta\lambda$, where

$$\cos \Delta\lambda = \frac{\cos \rho - \sin \phi_G \sin \phi}{\cos \phi_G \cos \phi}$$

This equation cannot provide high accuracy when ρ is small, but it can be algebraically converted into the better form:

$$\sin^2 \Delta\lambda = \frac{\sin^2 \rho - \sin \phi \, (\sin \phi - \cos \rho \sin \phi_G)}{\cos^2 \phi \cos^2 \phi_G}$$

$$- \frac{\sin \phi_G \, (\sin \phi_G - \cos \rho \sin \phi)}{\cos^2 \phi \cos^2 \phi_G}$$

If the visible range, $\lambda \pm \Delta\lambda$, is plotted against the independent variable η, Figure B, small eye-shaped apertures are found in the neighborhood of the intersection between the orbit and the latitude circle. A symmetric figure at $\eta > 90°$ exists, corresponding to the southbound intersection. These viewing eyes recur each time η increases another 360°, but the extent of nodal longitude that is viewable is the same each time. These are the only times during an orbit that the ϕ_G latitude circle is visible, subject to the nadir angle constraint.

The window angle constraint requires that the line-of-sight to a ground target make an angle, with respect to the window normal, μ, less than a specified μ_{MAX}. In the solar-inertial attitude, the window normal is aligned with the sun vector and looking away from the sun. For a specific satellite position, $\phi(\eta), \lambda(\eta)$, and a specific target position, ϕ_G, λ_G, that is within the visible range $\lambda \pm \Delta\lambda$, the window angle, μ, can be computed as follows:

$$\bar{R} = \left(R_e + h\right) \begin{pmatrix} \cos\lambda \cos \phi \\ \sin\lambda \cos \phi \\ \sin \phi \end{pmatrix} \qquad \bar{R}_G = R_e \begin{pmatrix} \cos \lambda_G \cos \phi_G \\ \sin \lambda_G \cos \phi_G \\ \sin \phi_G \end{pmatrix}$$

$$\bar{R}_{LOS} = \bar{R}_G - \bar{R}$$

$$R_s = \begin{pmatrix} \cos \lambda_s \cos \phi_s \\ \sin \lambda_s \cos \phi_s \\ \sin \phi_s \end{pmatrix} \qquad \cos \mu = \frac{\bar{R}_{LOS} \cdot \left(-\bar{R}_s\right)}{\left|R_{LOS}\right|}$$

By searching among all satellite positions that view the latitude circle and all ground target longitudes that are in view, the portion of the eye that also satisfies $\mu < \mu_{MAX}$ can be found. Depending on the position of the sun, this may exclude all, some, or none of the original eye. The two symmetric eyes, corresponding to ascending and descending intersections are not symmetric in this regard, and must be calculated separately.

The residual eyes, if any, define where a ground target must be in nodal longitude vs η if it is to be photographed. The path of a desired ground target can be calculated as λ_G vs η, and if this path intersects the eye, photography can be accomplished at any time the ground site lies within the nodal longitude bounds of the eye.

Perturbation Effects

The gravitational potential of the oblate earth can be written to first order as:

$$U = \frac{\mu}{R}\left[1 + \frac{J_2}{2}\left(\frac{R_e}{R}\right)^2\left(3\sin^2\phi - 1\right) + \ldots\right]$$

where

$$\mu = 1.407646 \times 10^{16}\ \frac{ft^3}{sec^2}$$

$$J_2 = 1082.7 \times 10^{-6} \quad .$$

If the J_2 term (and higher) were absent, the orbit would remain a perfect ellipse with an inertially fixed plane. The period to make one revolution, returning exactly to the starting point, would be

$$\tau_o = \sqrt{\frac{\mu}{a_o^3}}$$

where the semi-major axis a_o is equal to the radius of the circular orbit.

The presence of the J_2 term introduces periodic variations into all orbit elements which we will ignore, and secular variations into Ω, the nodal angle, and ω, the argument of perigee. Several different periods can also be defined, including the anomalistic period τ_a, the time to move from one perigee to the next; and nodal period τ_N, the time to move from one ascending node to the next.

$$\tau_a = 2\pi \sqrt{\frac{\bar{a}^3}{\mu}} \left\{ 1 + \frac{3J_2}{(1-e^2)^{3/2}} \left(\frac{R_e}{\bar{a}}\right)^2 \left(\frac{3\cos^2 i - 1}{8}\right) \right\}$$

$$\tau_N = 2\pi \sqrt{\frac{\bar{a}^3}{\mu}} \left\{ 1 - 3J_2 \left(\frac{R_e}{\bar{a}}\right)^2 \left(\frac{7\cos^2 i - 1}{8}\right) \right\}$$

where

$$\bar{a} = a_o \left\{ 1 - \frac{3J_2}{2} \left(\frac{R_e}{p}\right)^2 \left(1 - \frac{3}{2}\sin^2 i\right) \sqrt{1 - e^2} \right\} .$$

The use of $\bar{a}$ in place of a_o reflects the fact that the gravitational acceleration experienced by the satellite is enhanced, on the average, by the J_2 term, requiring the satellite to go faster to stay up at a radius a_o. The extra additive terms in the periods are due to the motion of the reference point: forward for the perigee, and backward for the node.

Integration of the differential equation for $\frac{d\Omega}{dt}$ over a full revolution, holding other elements constant, yields a change in position of the node

$$\Delta\Omega = -3\pi J_2 \left(\frac{R_e}{p}\right)^2 \cos i, \quad \left(\frac{\text{rad}}{\text{rev}}\right) .$$

The average rate of nodal regression is therefore

$$\bar{\dot{\Omega}} = \frac{\Delta\Omega}{\tau_o} .$$

Thus, in inertial space the node moves eastward at about a rate of -5 deg/day (i.e., westward) while the earth rotates eastward at a rate

$$\omega_e = 360 \times \frac{366.25}{365.25} \text{ deg/day.}$$

Relative to the nodal coordinate system, a ground site will move eastward at a rate

$$\dot{\lambda}_G = \omega_e - \bar{\dot{\Omega}}$$

It is convenient to define a nodal day which lasts for a time (somewhat shorter than a normal solar day)

$$T_{ND} = \frac{360°}{\omega_e - \bar{\dot{\Omega}}}$$

and which starts rather arbitrarily at the instant the selected ground site is at the meridian of the ascending node. Then

$$\lambda_G = o + \dot{\lambda}_G t$$

where t is time into the nodal day.

This daily motion of the ground site can be related to the position of the satellite in its orbit. $\eta = \eta_o + \dot{\eta}t$ where η_o is the initial position of the satellite when t = o and

$$\dot{\eta} = \frac{360°}{\tau_N}$$

Solving both equations to eliminate t, we obtain the basic relation between ground site nodal longitude and satellite position:

$$\lambda_G = \frac{\dot{\lambda}_G}{\dot{\eta}} \left(\eta - \eta_o \right) \quad .$$

This straight line, plotted as λ_G vs η, may or may not intersect the ground site visibility eyes previously derived, depending entirely on η_o, the satellite position at the beginning of the nodal day. On each successive day η_o will be different because the orbit period is not commensurate with the nodal day:

$$\eta_{o_i} = \left(\eta_{o_{i-1}} + \dot{\eta}\, T_{ND} \right) \text{ modulo } 360^\circ .$$

Finding photographic opportunities is then reduced to finding days on which η_o falls in a range that causes the ground site longitude to intersect one of the visibility eyes.

Sun's Position and Lighting

The sun may be regarded as circling the earth once per year on an orbit that is inclined $\varepsilon = 23.5^\circ$ to the equator. The satellite orbit node is Ω deg east of the sun's ascending node and Ω increases at the previously derived rate $\dot{\bar{\Omega}}$ due to the nodal regression of the satellite orbit. The sun's position relative to the satellite orbit node is calculated from

$$\sin \phi_s = \sin \eta_s \sin \varepsilon$$

$$\tan \lambda'_s = \tan \eta_s \cos \varepsilon$$

$$\lambda_s = \lambda'_s - \left(\Omega_o + \dot{\bar{\Omega}}\, D \right)$$

where

$$\eta_s = 360° \times \frac{D}{365.25}$$

D = No. of days past the vernal equinox

Ω_o = initial node angle of orbit relative to sun node at D = 0.

The sun's motion, therefore, consists of an annual oscillation in ϕ_s plus an eastward, nearly linear, drift in λ_s of about 6 deg/day; 1 deg/day from λ_s' and 5 deg/day from nodal regression.

The solar lighting angle is the central angle between the sun's position, ϕ_s, λ_s, and the point of intersection between the orbit and latitude circle ϕ_G. The longitude of the intersection is

$$\lambda_i = \sin^{-1}\left(\frac{\tan \phi_G}{\tan i}\right) .$$

The solutions on either side of 90° should be used for the ascending and descending intersections. Then the solar lighting angle is

$$\Theta = \cos^{-1}\left(\cos \phi_G \cos \phi_s \cos \left(\lambda_i - \lambda_s\right) + \sin \phi_G \sin \phi_s\right) .$$

The angle between the sun vector and the orbit plane can also be computed:

$$\beta = \sin^{-1}\left(\sin \phi_s \cos i - \cos \phi_s \sin \lambda_s \sin i\right) .$$

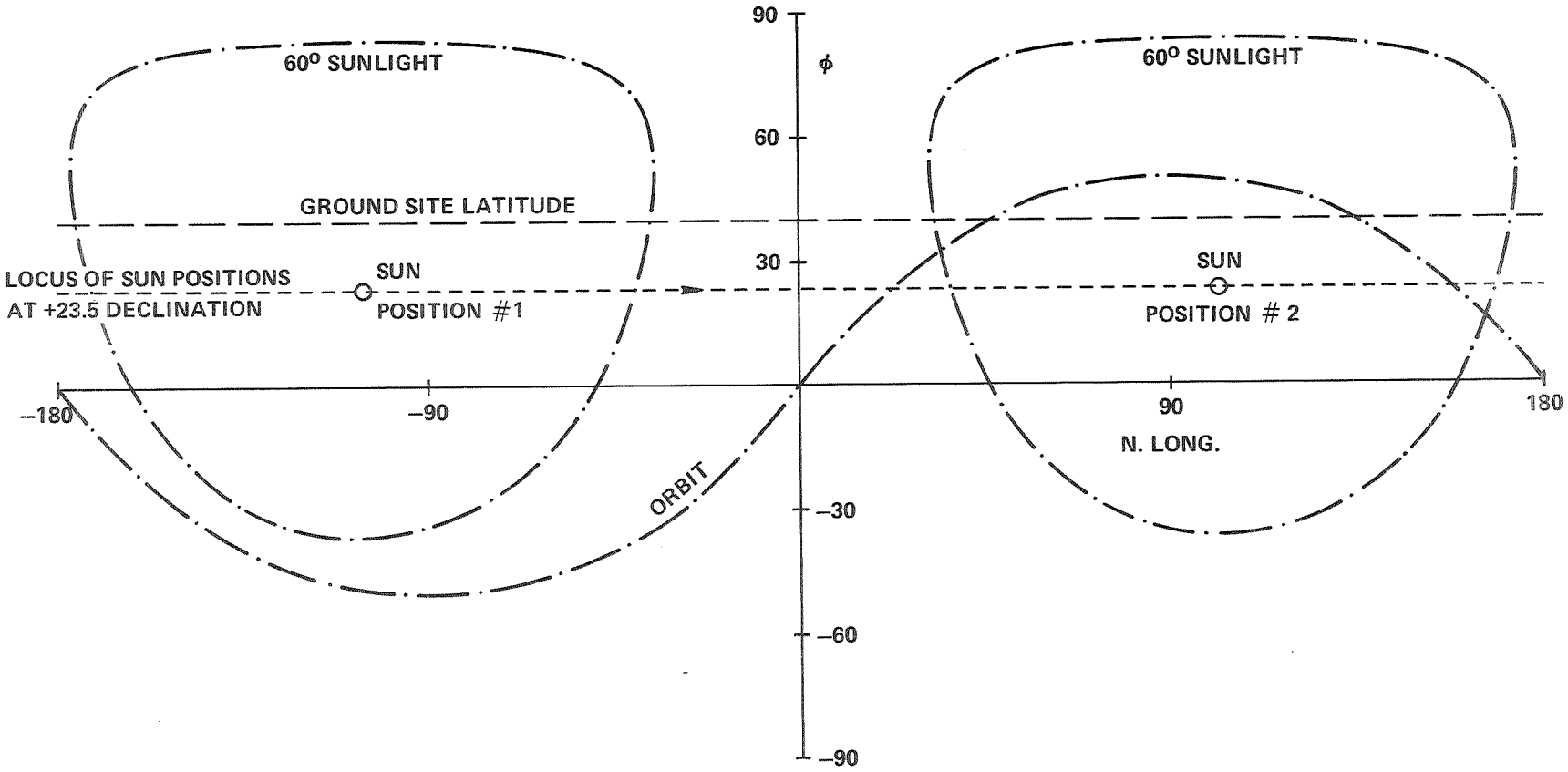

FIGURE 1 - ORBIT PLANE GEOMETRY

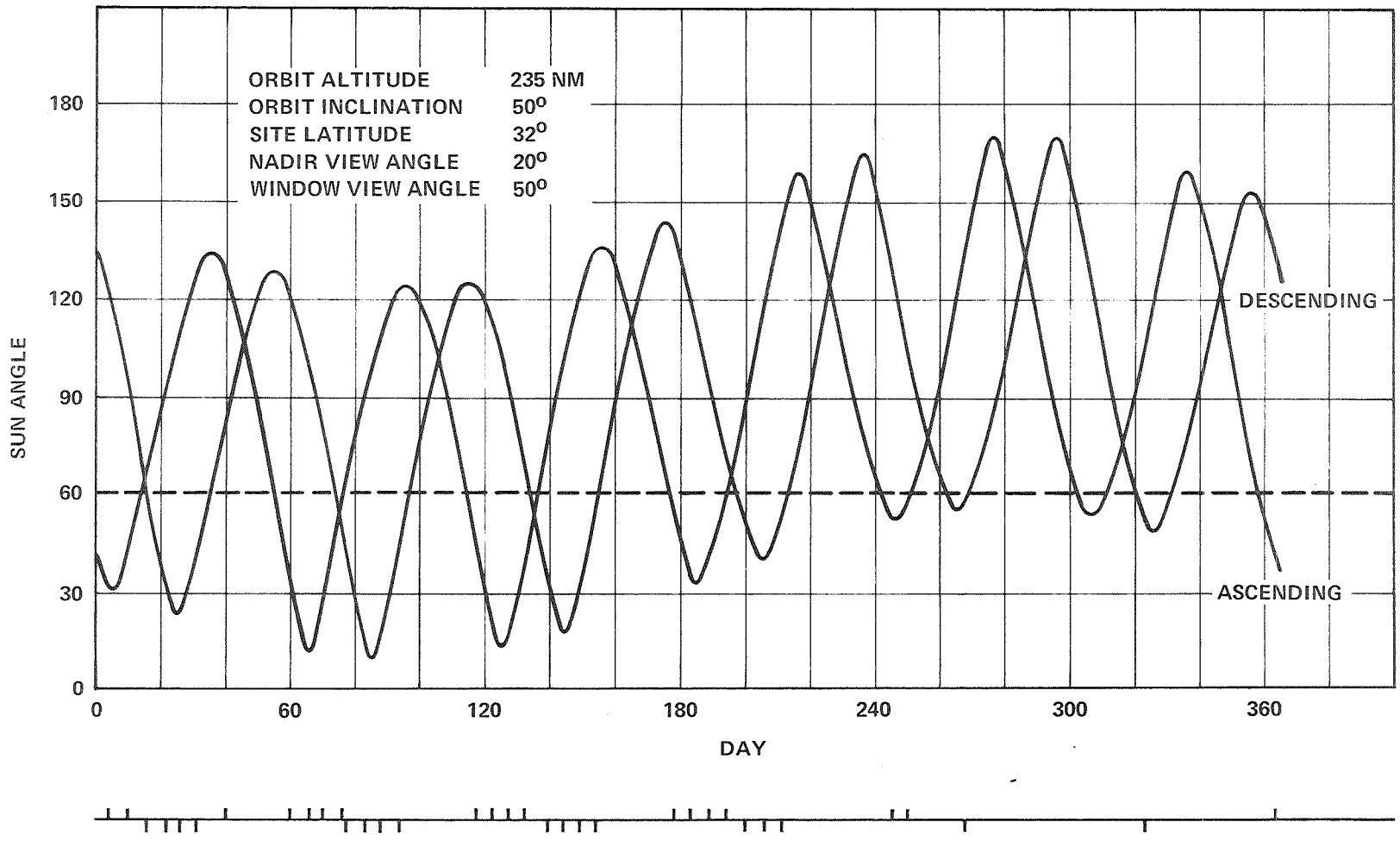

FIGURE 2 - SUN ILLUMINATION ANGLE & VIEWING OPPORTUNITIES VS. DAY OF YEAR

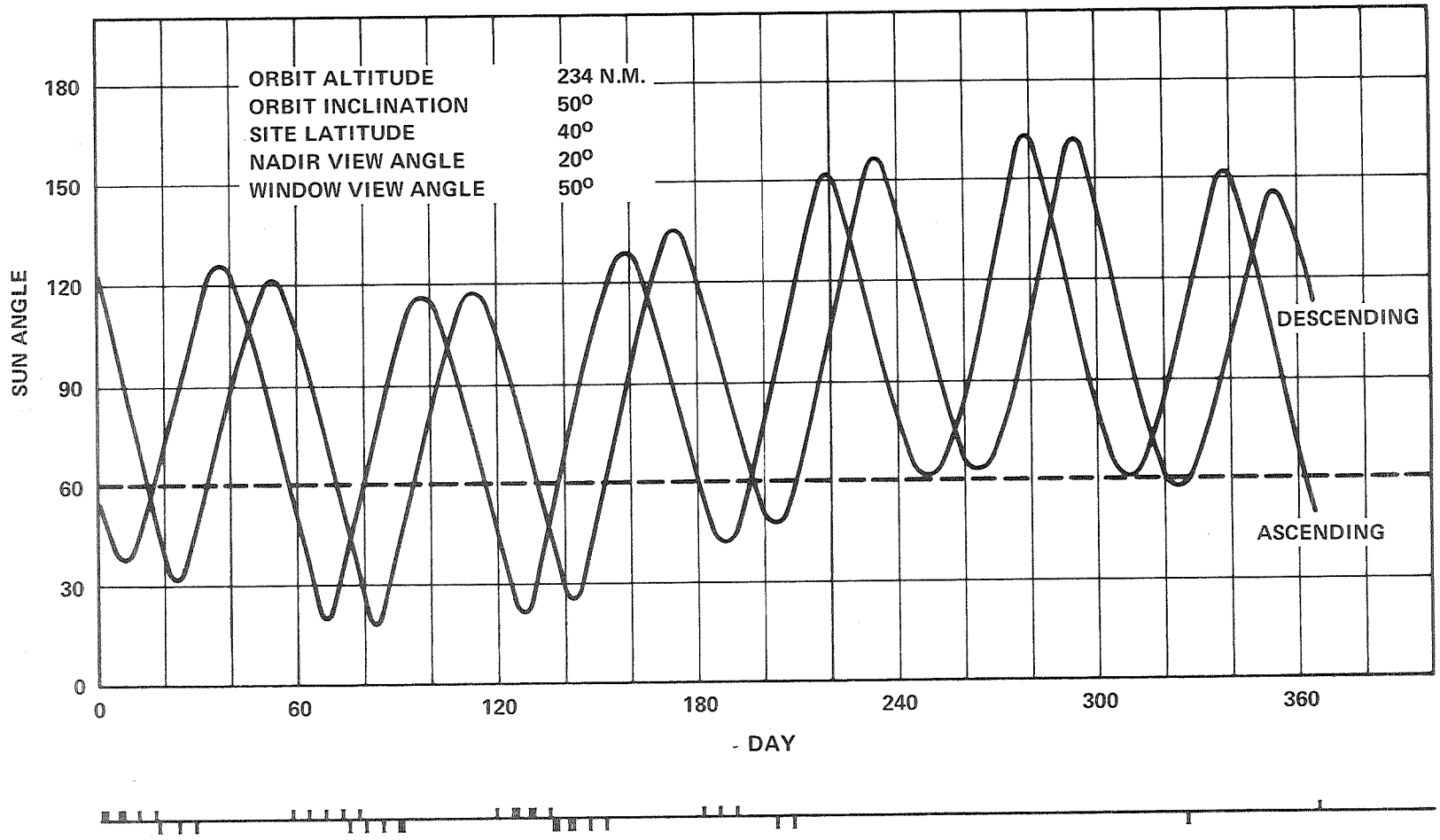

FIGURE 3 - SUN ILLUMINATION ANGLE & VIEWING OPPORTUNITIES VS. DAY OF YEAR

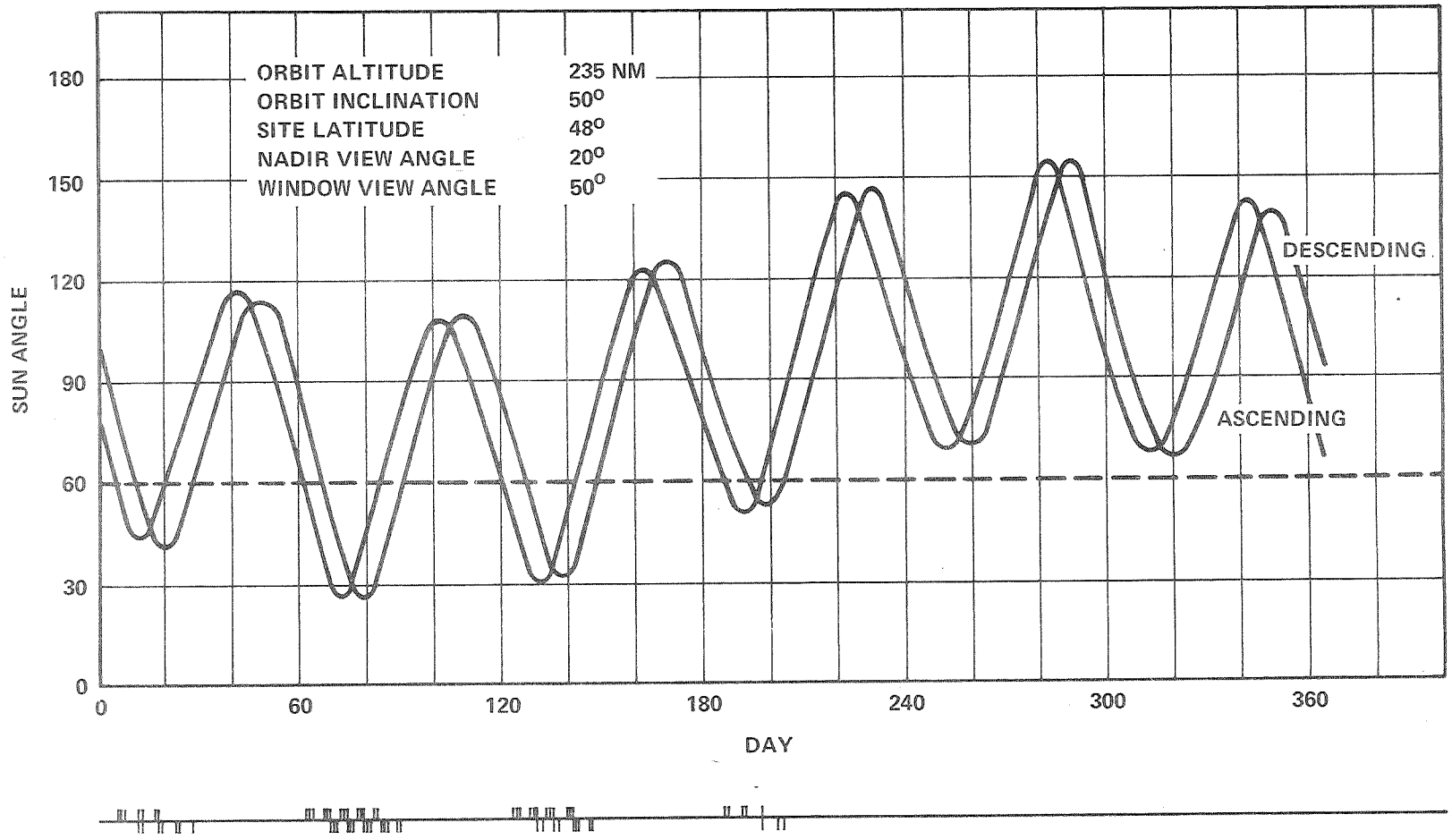

FIGURE 4 - SUN ILLUMINATION ANGLE & VIEWING OPPORTUNITIES VS. DAY OF YEAR

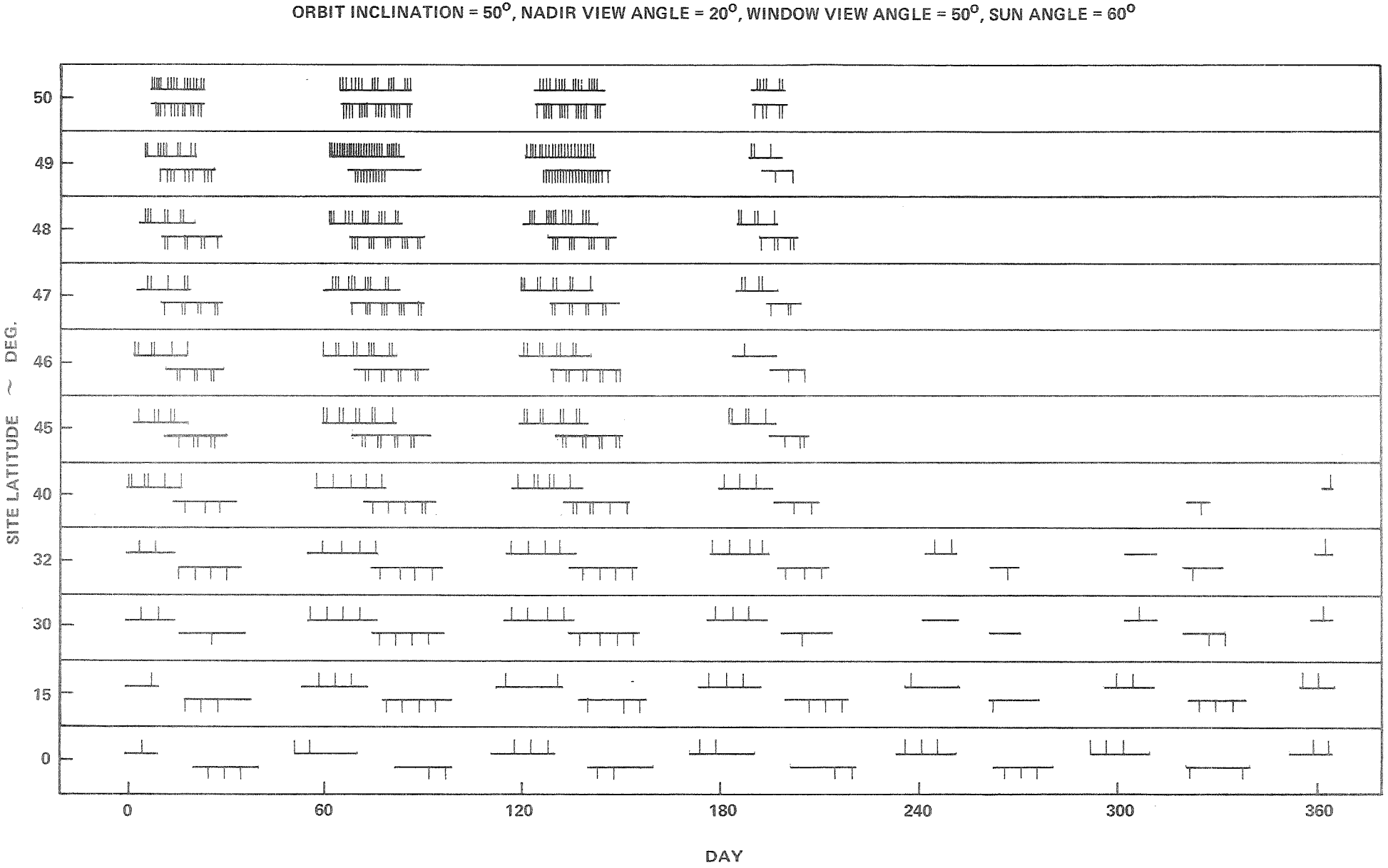

FIGURE 5 - VIEWING OPPORTUNITIES VS. DAY OF YEAR

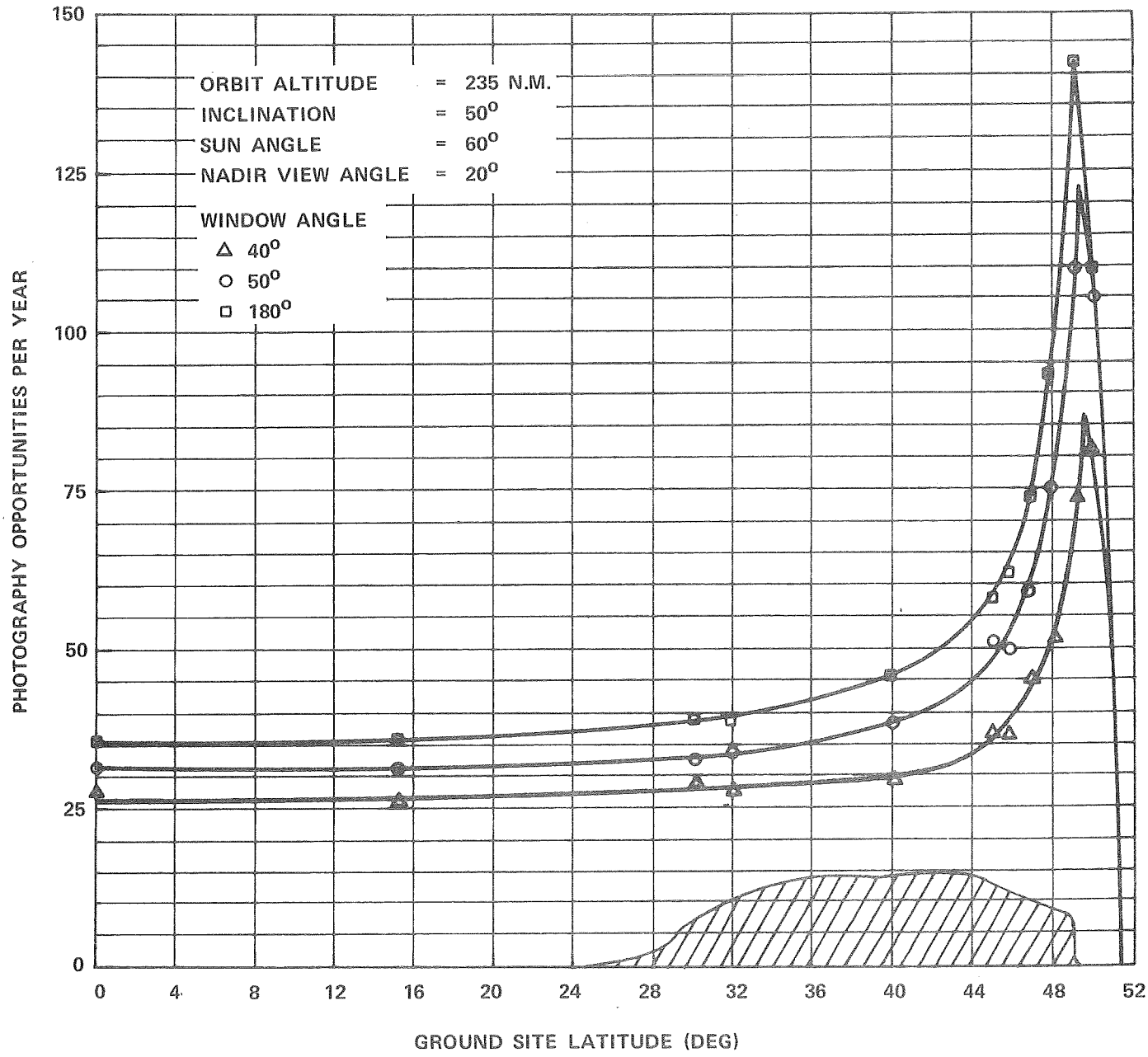

FIGURE 6 - PHOTOGRAPHY OPPORTUNITIES vs. SITE LATITUDE

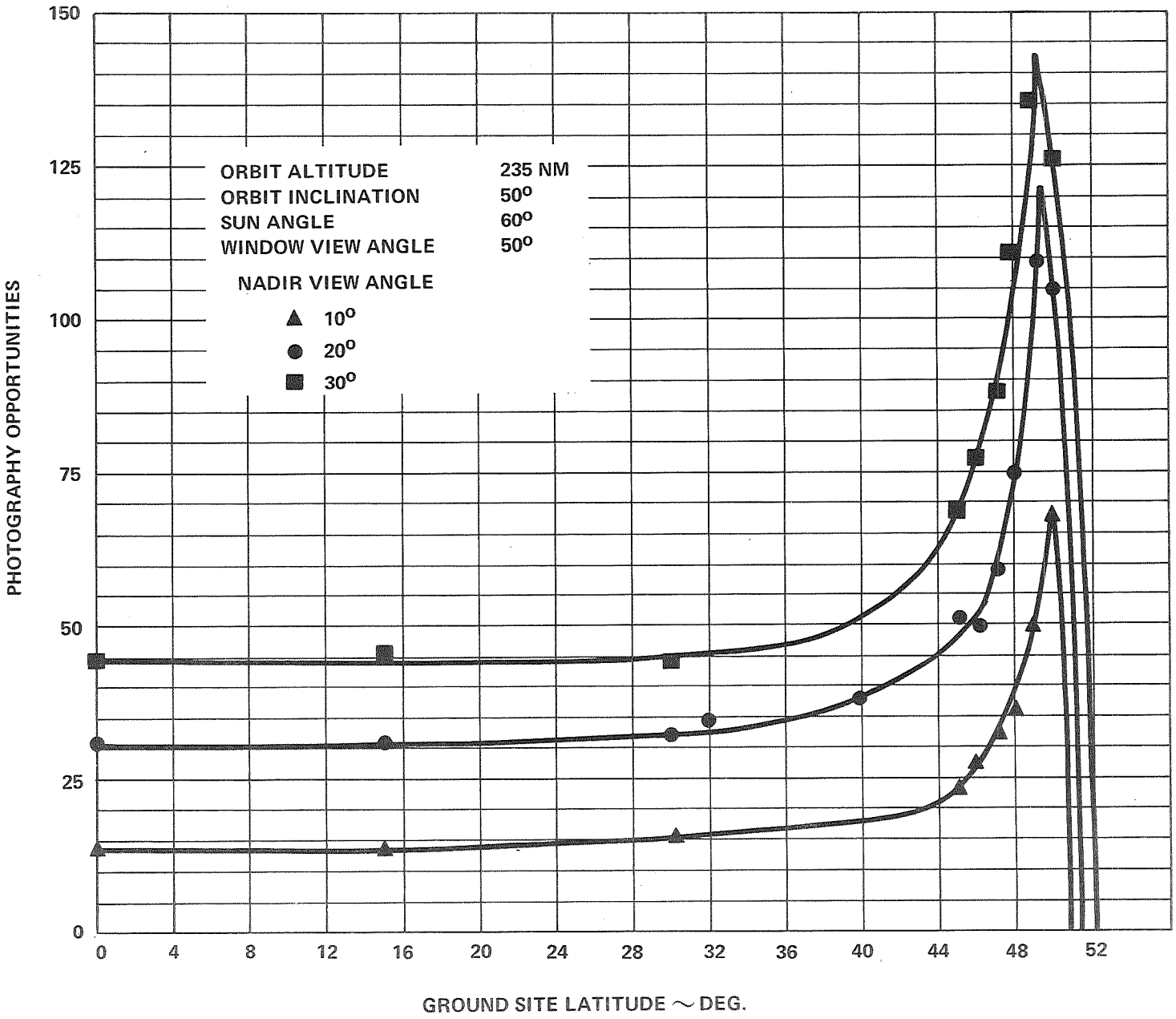

FIGURE 7 - ANNUAL PHOTOGRAPHY OPPORTUNITIES VS. SITE LATITUDE

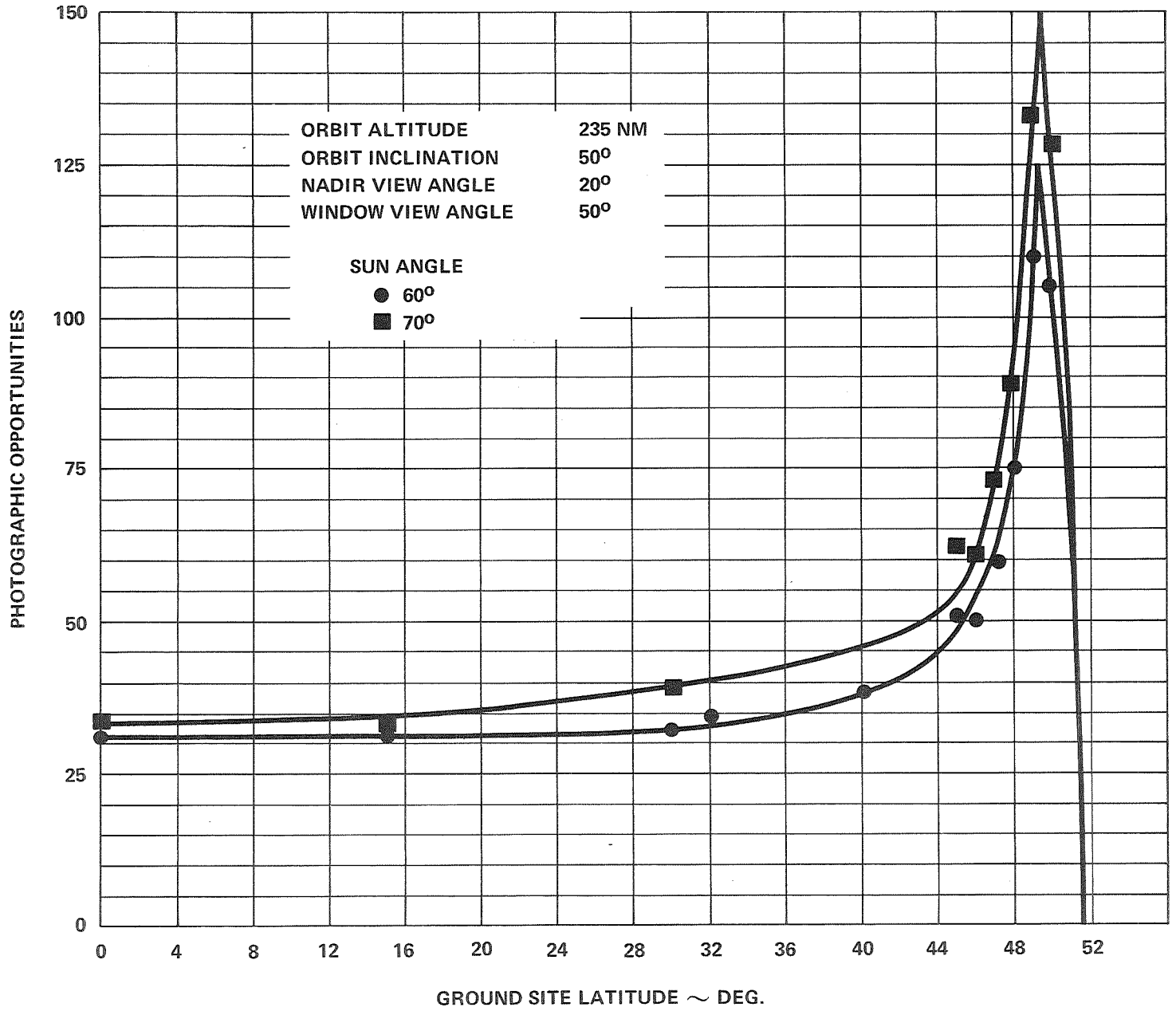

FIGURE 8 - ANNUAL PHOTOGRAPHY OPPORTUNITIES VS. SITE LATITUDE

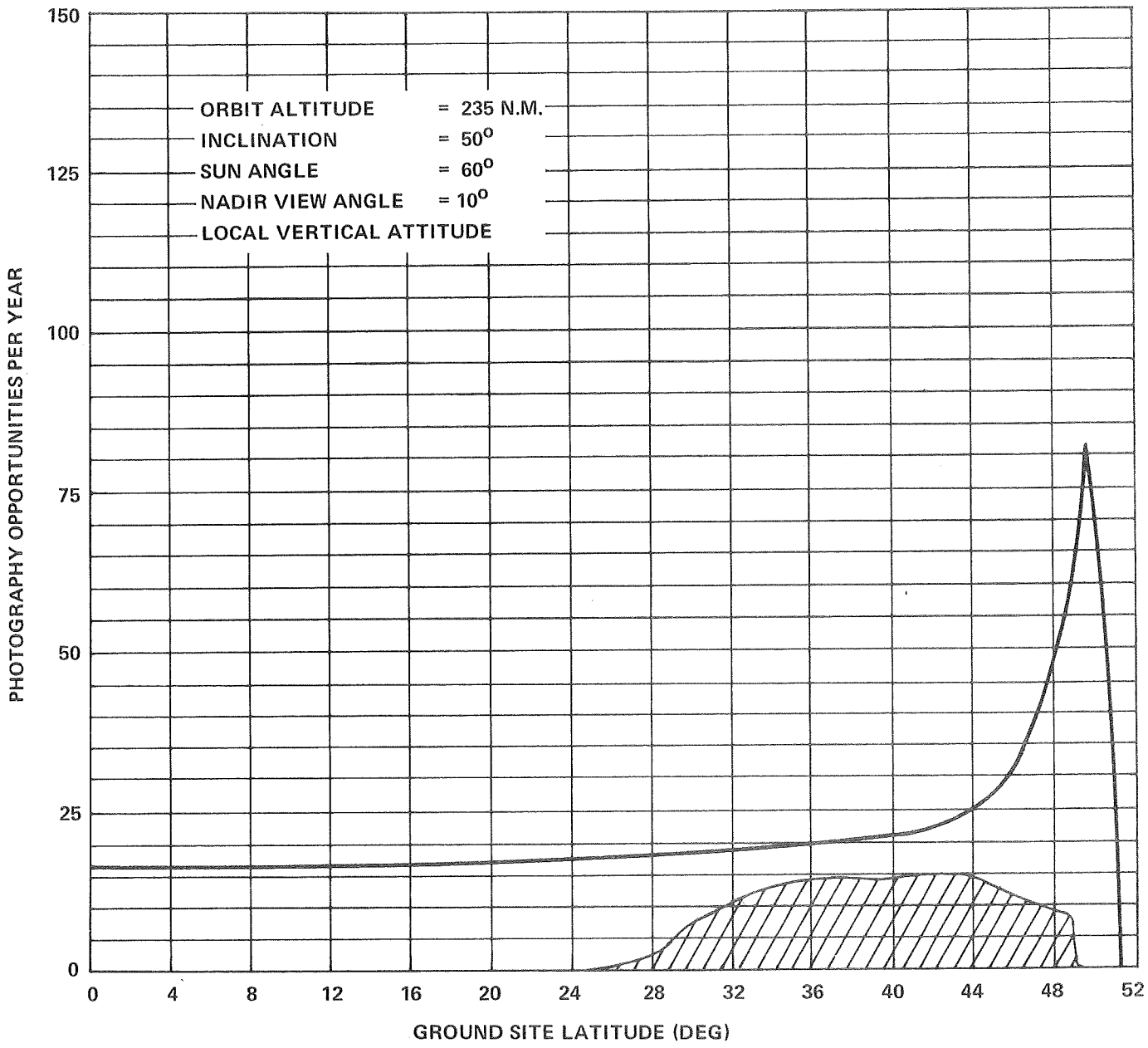

FIGURE 9 - PHOTOGRAPHY OPPORTUNITIES vs. SITE LATITUDE

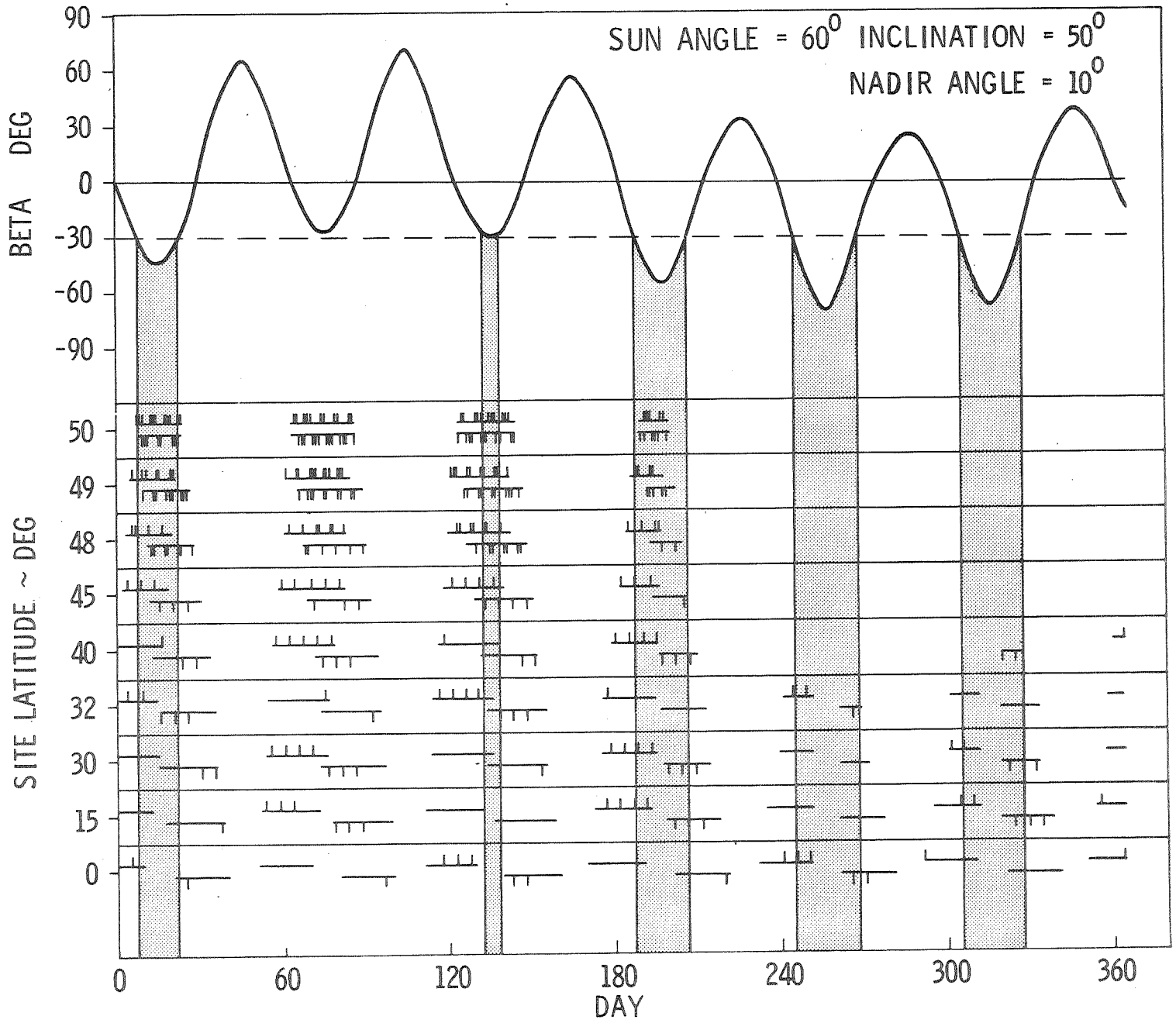

FIGURE 10 - LOCAL VERTICAL PHOTOGRAPHY OPPORTUNITIES

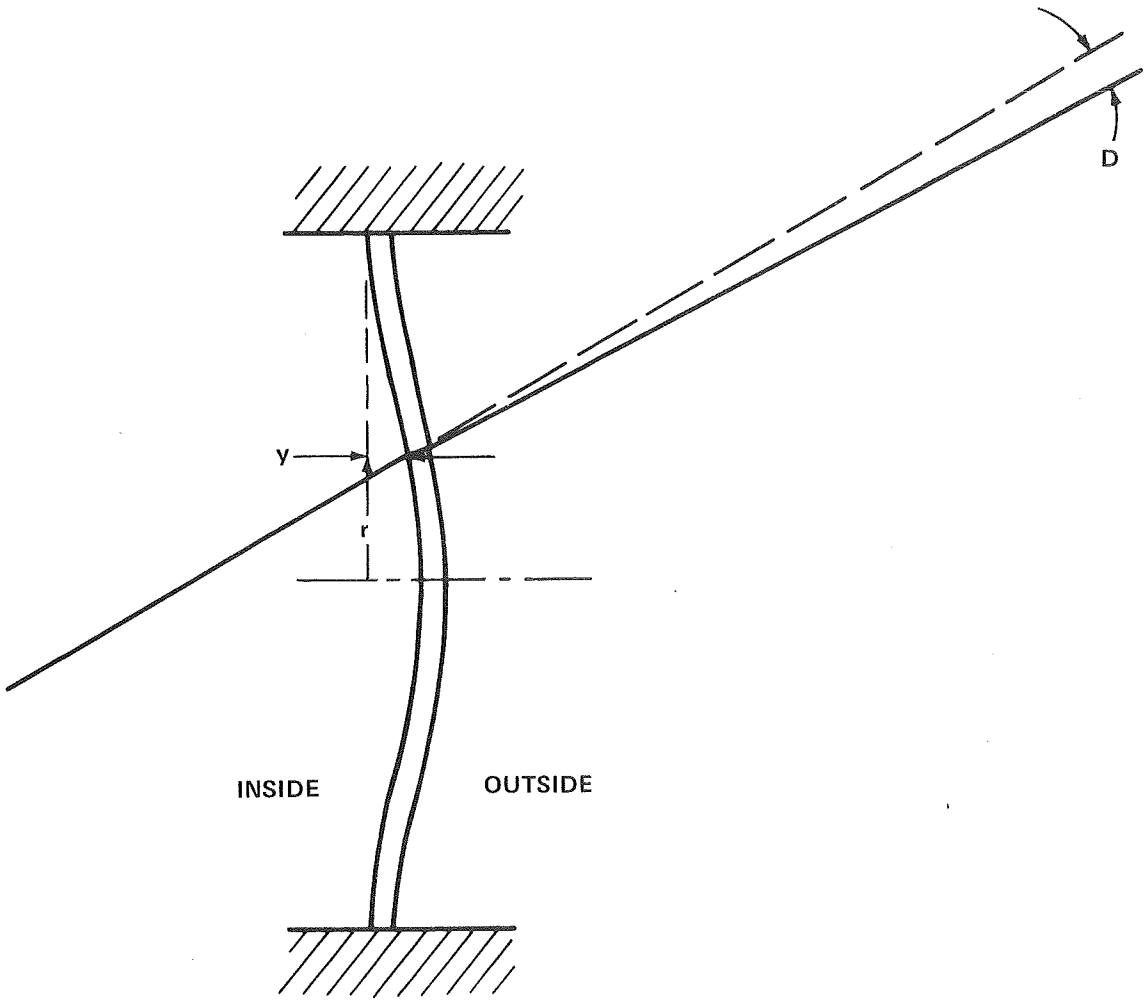

FIGURE 11 - WINDOW DEFORMATION UNDER PRESSURIZATION

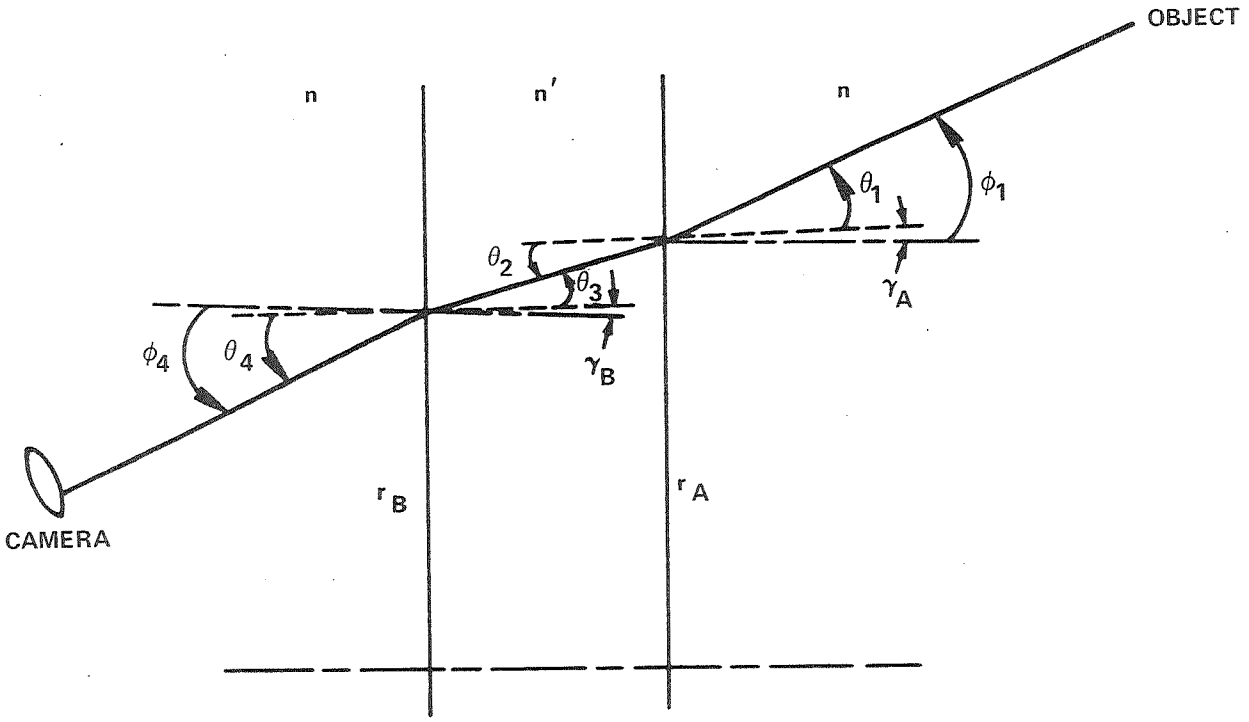

RAY TRACING ANGLES

Θ'S ARE MEASURED FROM NORMAL TO SURFACE

ϕ'S ARE MEASURED FROM PRINCIPLE AXIS

γ'S ARE TILT OF MORMAL'S RELATIVE TO PRINCIPLE AXIS

FIGURE 12 - RAY GEOMETRY

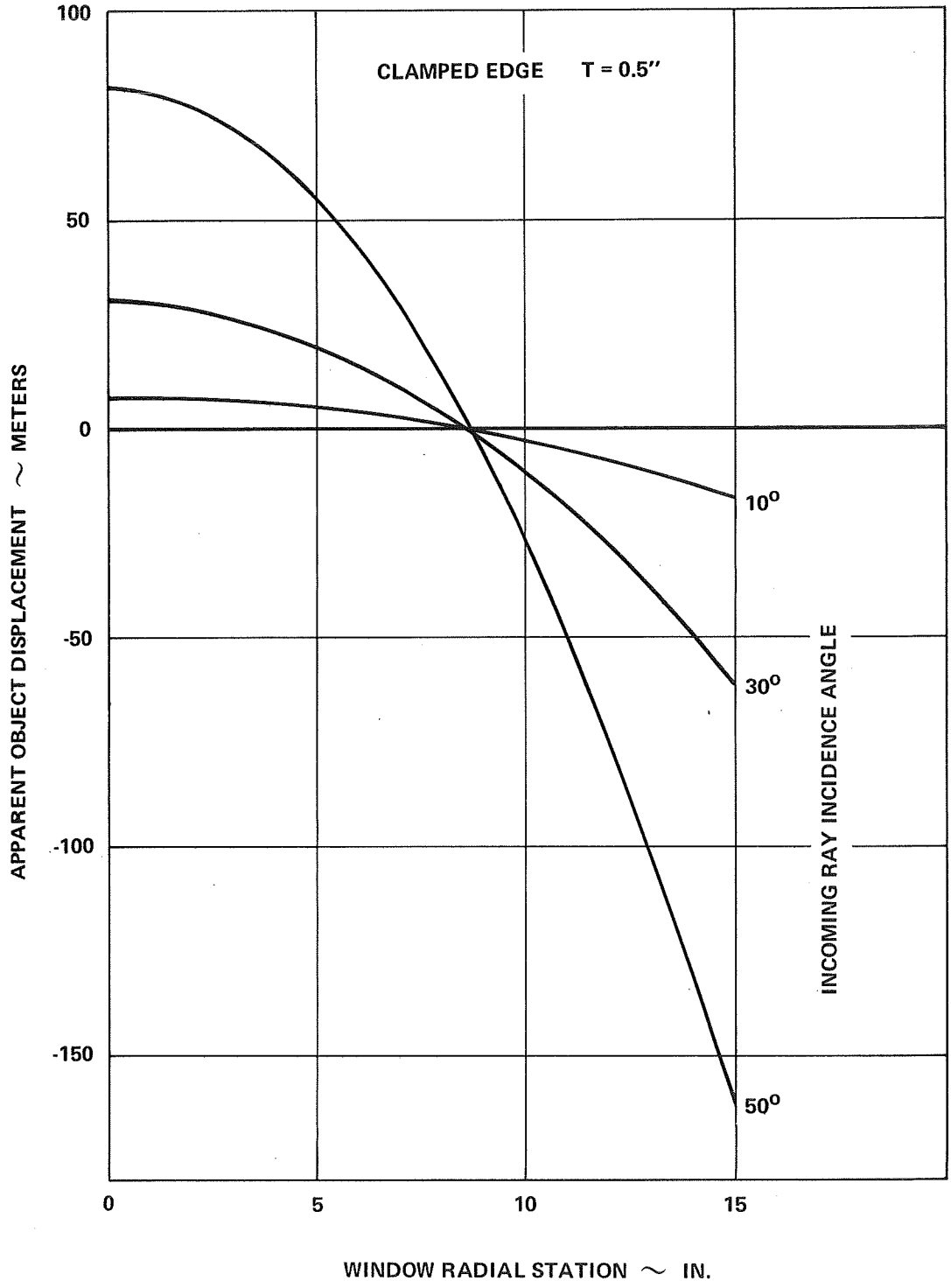

FIGURE 13 - VARIATION OF APPARENT OBJECT DISPLACEMENT

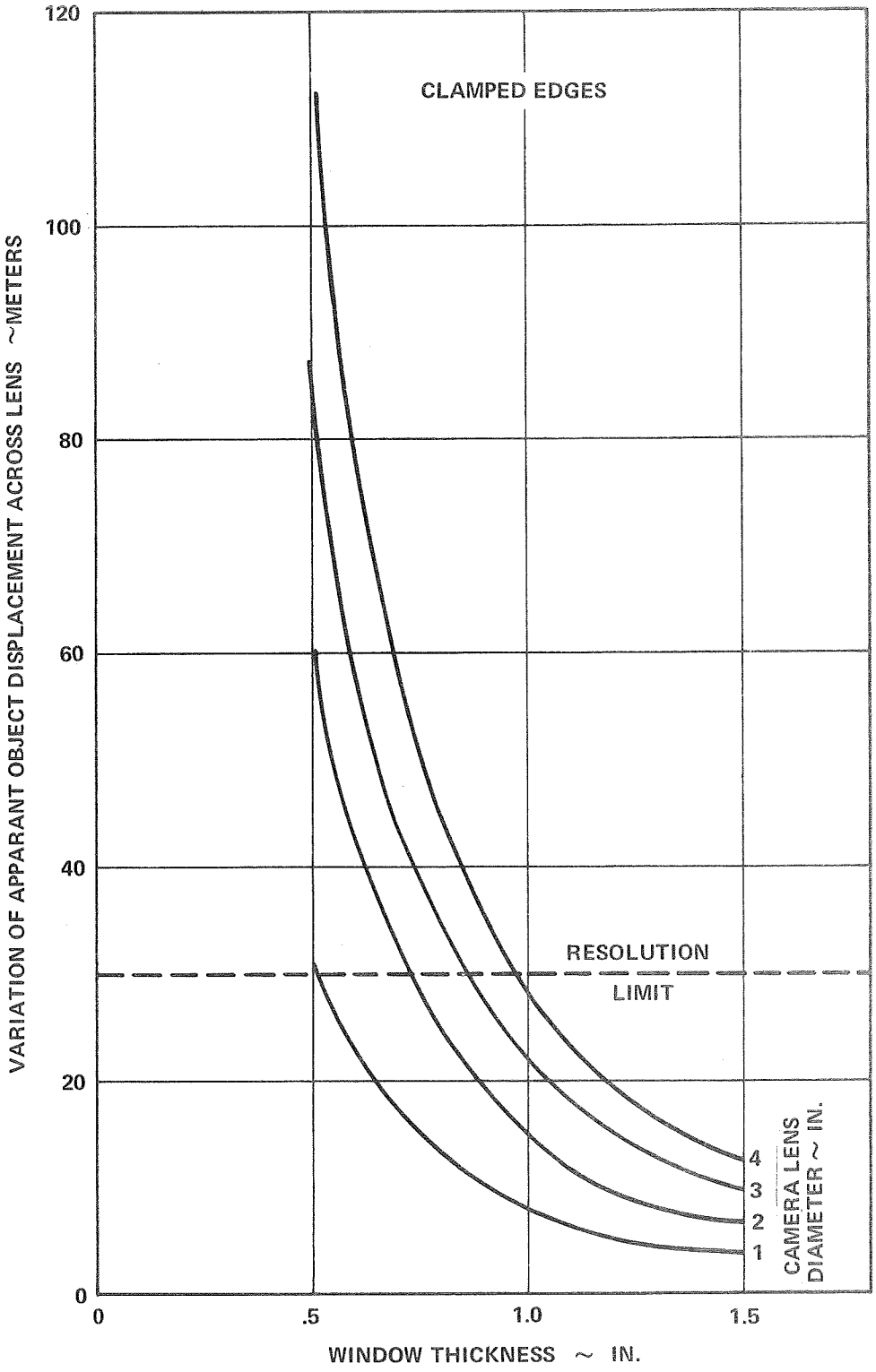

FIGURE 14 - MAXIMUM APPARENT OBJECT DISPLACEMENT ACROSS LENS

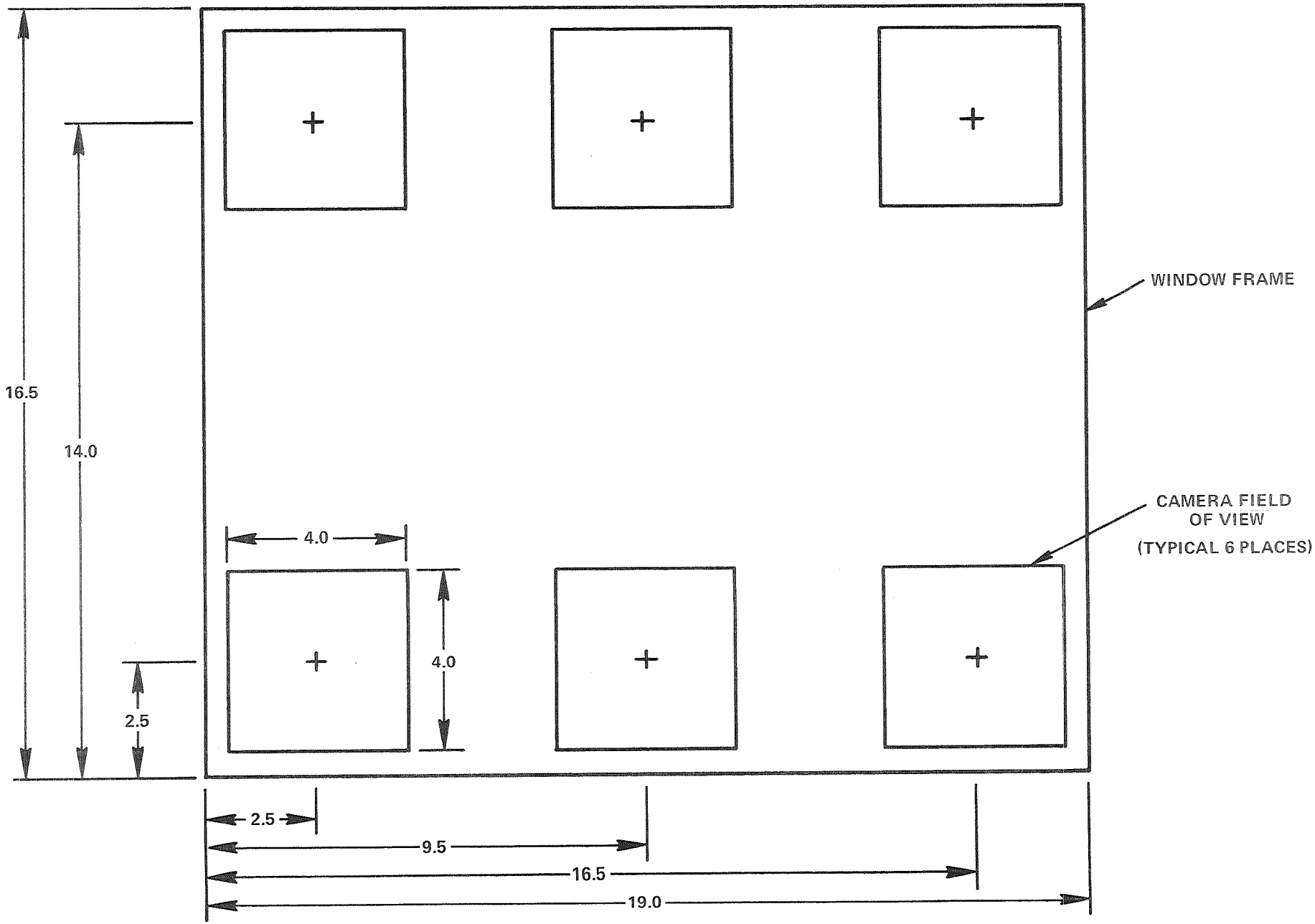

FIGURE 15 - CAMERA RACK GEOMETRY

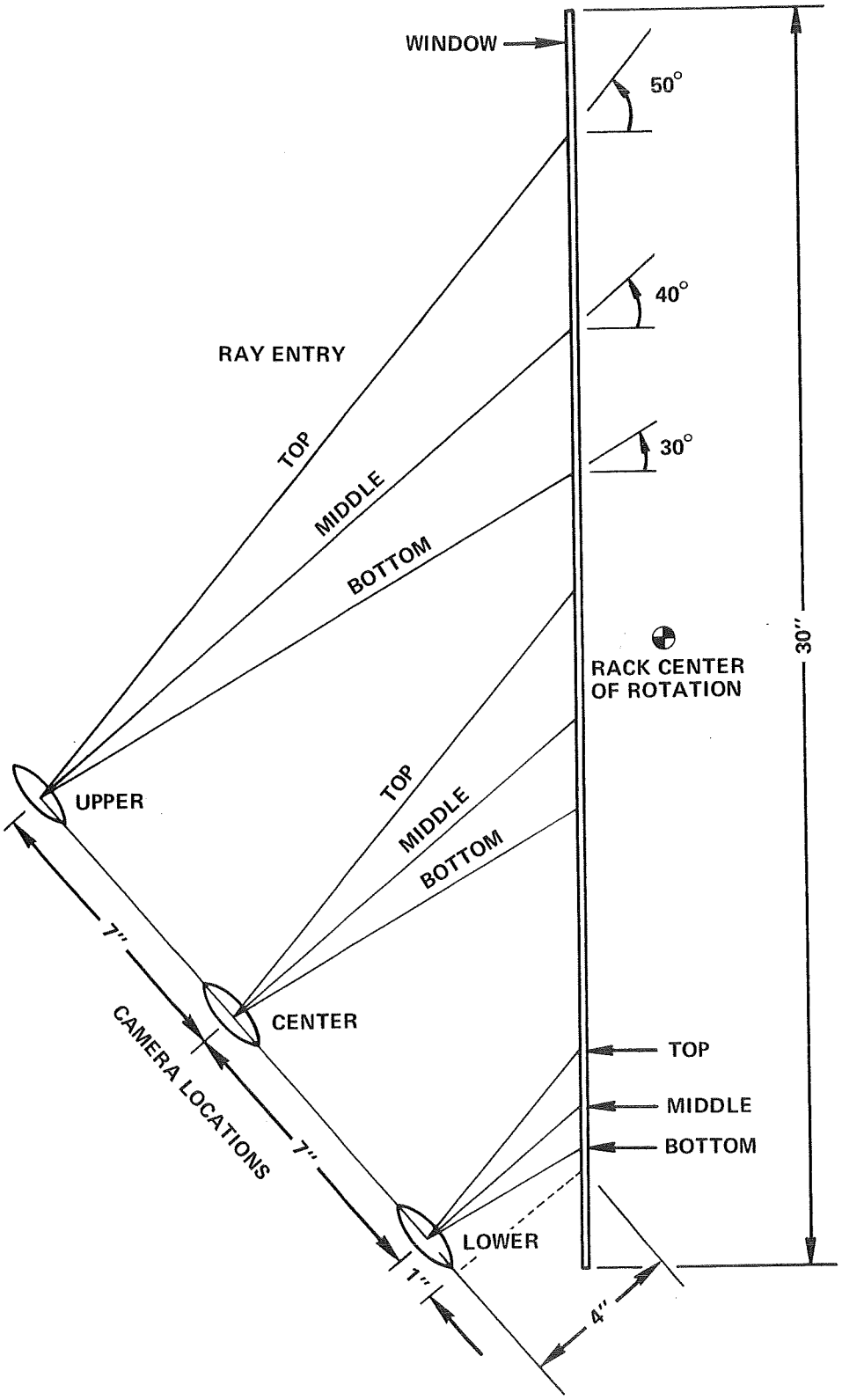

FIGURE 16 - CAMERA/WINDOW GEOMETRY

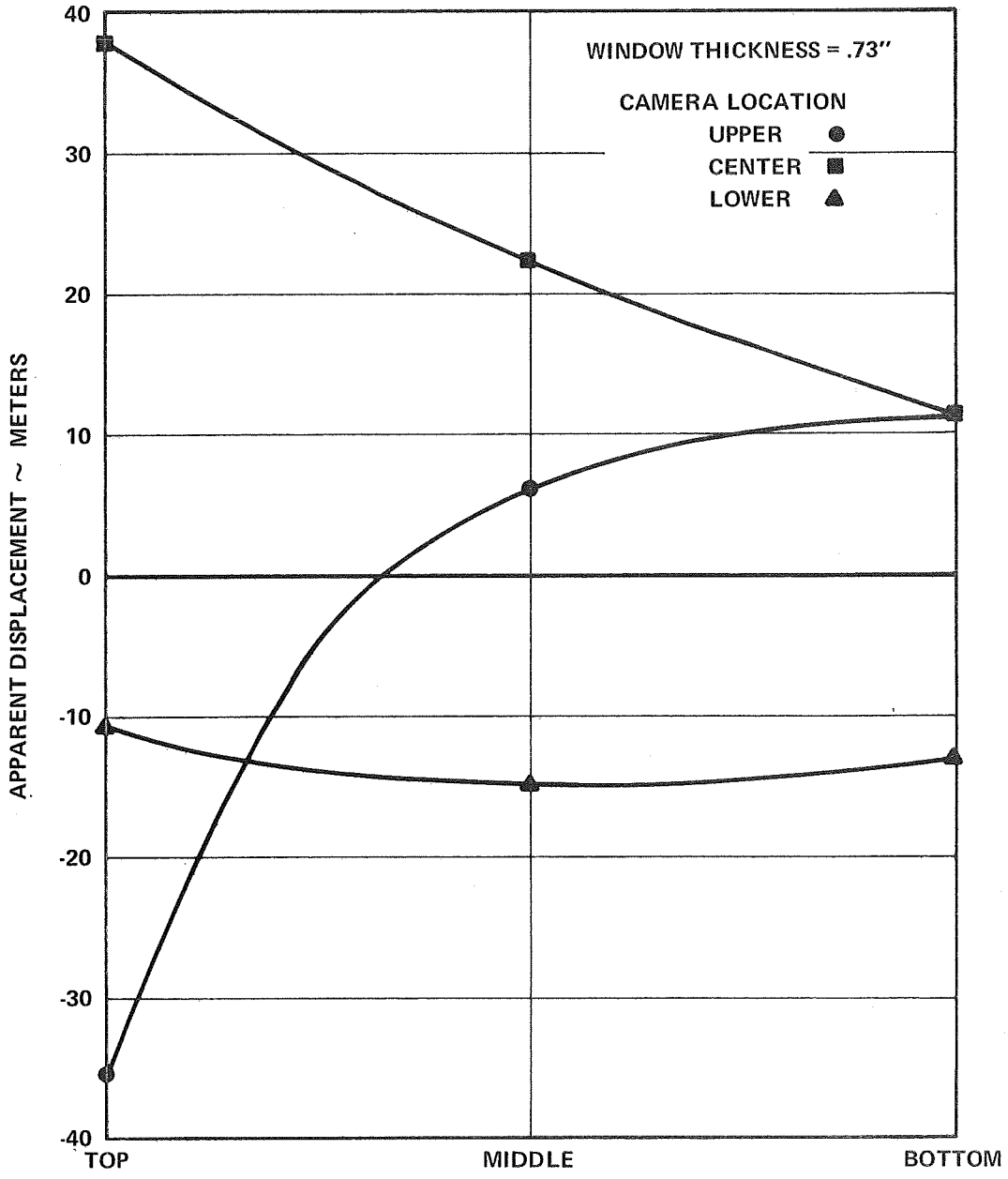

FIGURE 17 - REGISTRATION VARIATION ACROSS PICTURE AREA

CAMERA RACK PIVOT POINT 2" OUTSIDE OF WINDOW INNER SURFACE
REQUIRED WINDOW DIMENSION = 27.4" x 25.8"; PIVOT ARM LENGTH = 14.9"

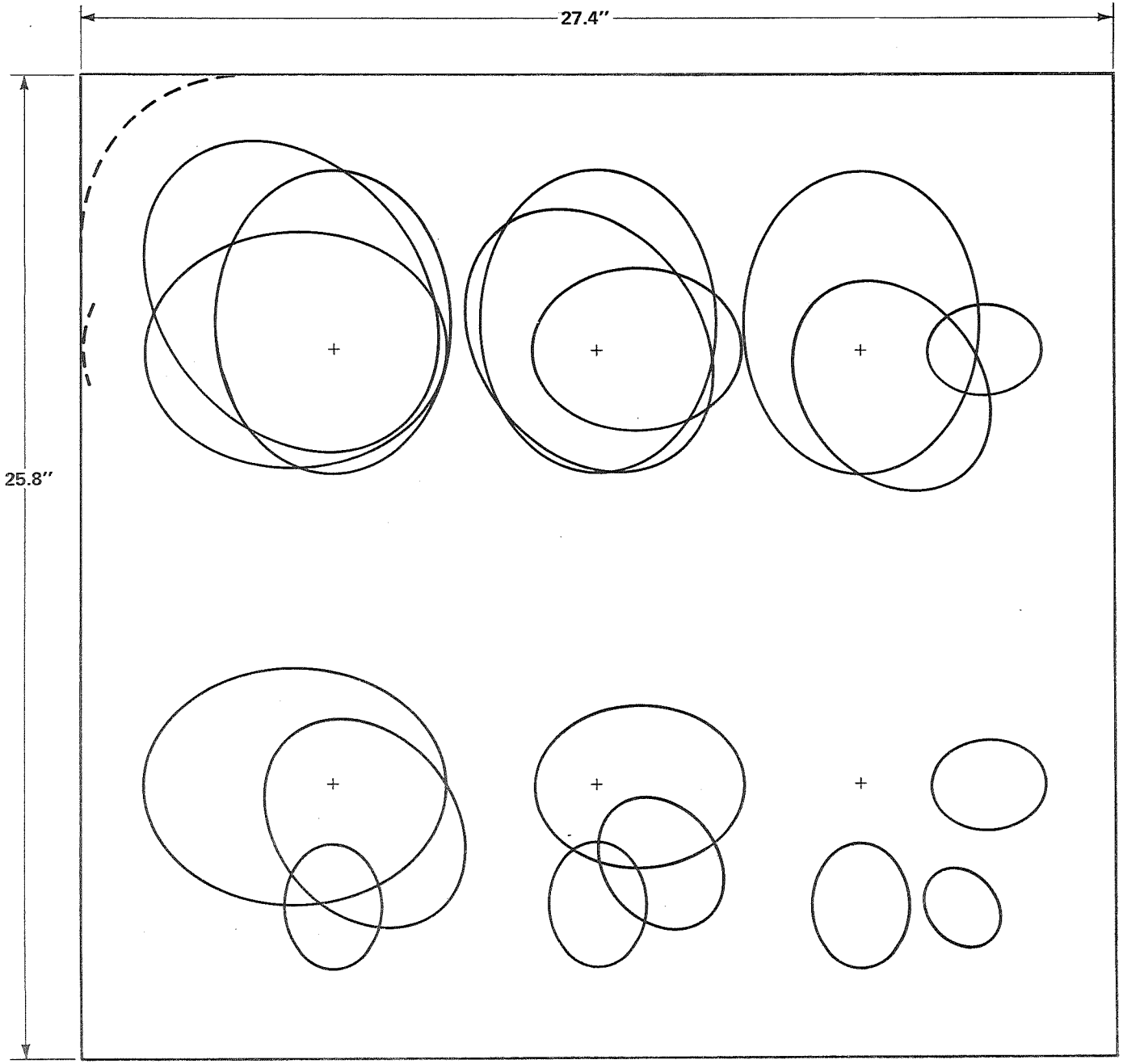

FIGURE 18 - RAY PENETRATION PATTERNS

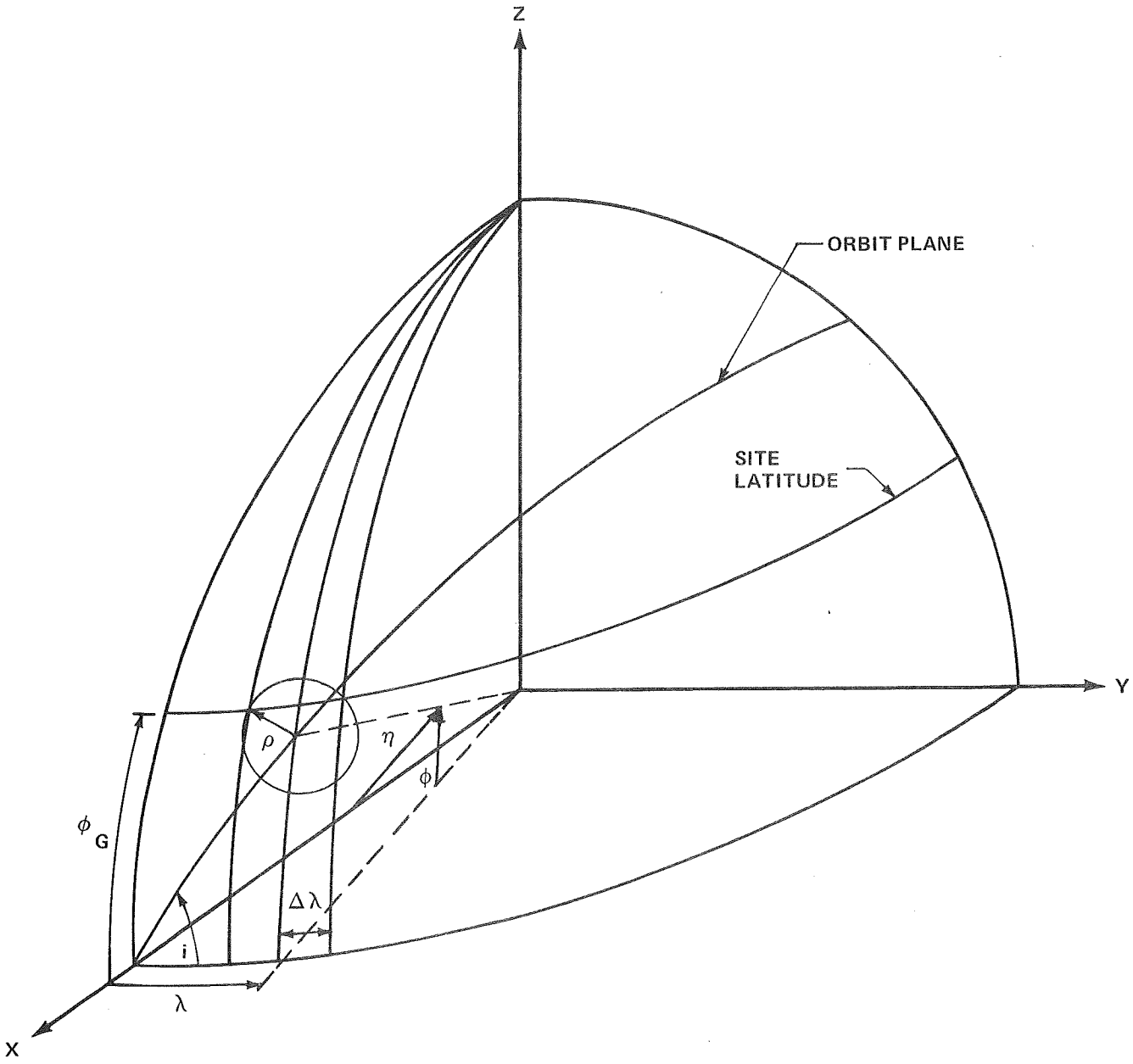

FIGURE A, COORDINATE SYSTEM

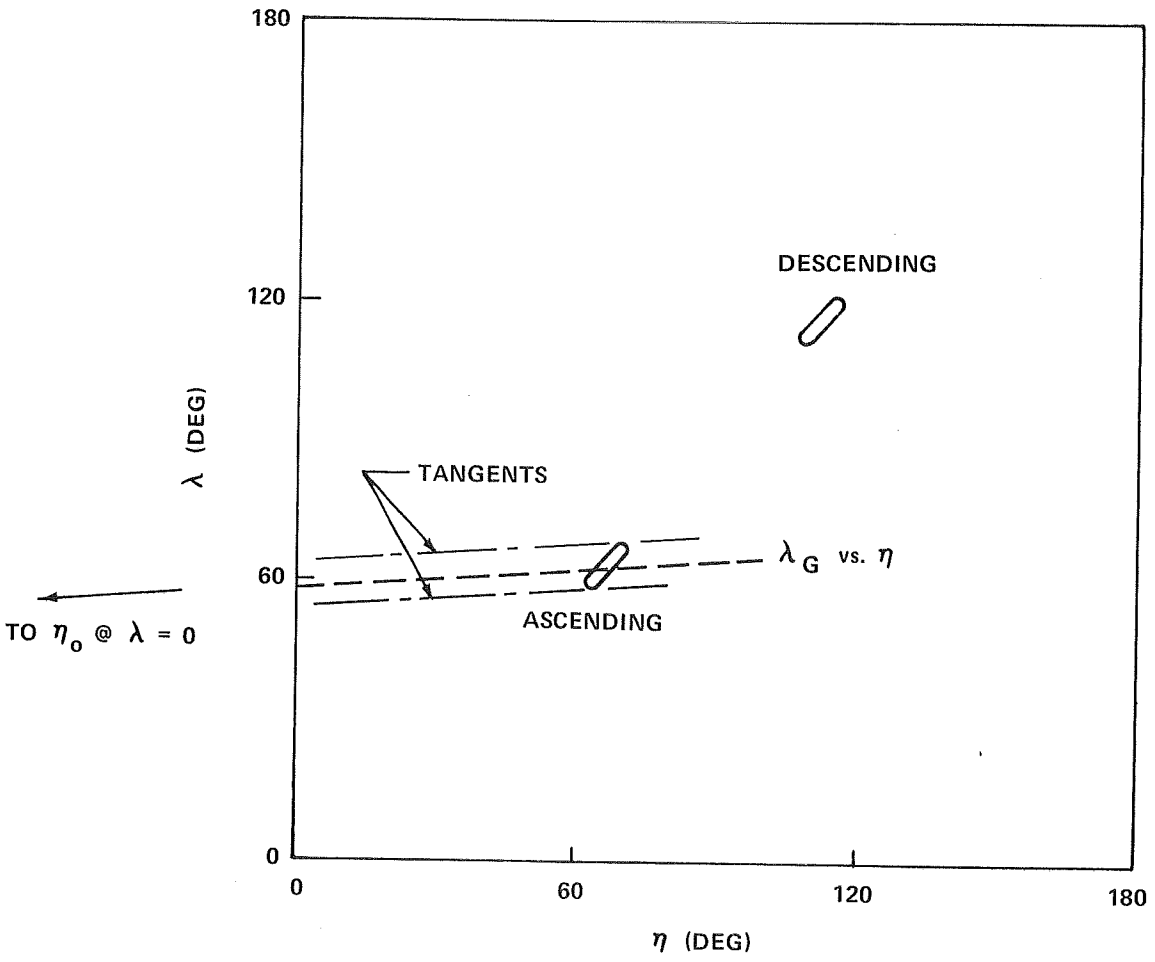

FIGURE B - VISIBILITY REGIONS

BELLCOMM, INC.

Subject: Photography of Ground Sites from AAP Orbit - Case 610

From: D. A. De Graaf
E. W. Radany

DISTRIBUTION LIST

NASA Headquarters

H. Cohen/MLR
J. H. Disher/MLD
W. B. Evans/MLO
L. K. Fero/MLV
J. P. Field, Jr./MLP
T. E. Hanes/MLA
T. A. Keegan/MA-2
J. G. Lundholm/MLA
M. Savage/MLT
W. C. Schneider/ML

MSC

A. A. Bishop/KM
A. L. Grandfield/TF
G. L. Hunt/FM13
W. E. Koons/FA
F. C. Littleton/KM
R. M. Machell/KF
R. O. Piland/TF
R. F. Thompson/KA

MSFC

L. F. Belew/PM-AA-MGR
J. W. Cremin/S&E-AERO-DA
C. C. Hagood/S&E-AERO-P
G. B. Hardy/PM-AA-EA
R. C. Lester/S&E-AERO-P
J. W. Thomas/PM-S/AA
R. E. Tinius/S&E-AERO-P
J. H. Waite/PM-S/AA

Martin-Marietta Corp.

E. F. Bjoro
T. Heaton

Bellcomm, Inc.

A. P. Boysen, Jr.
D. R. Hagner
W. G. Heffron
J. J. Hibbert
N. W. Hinners
B. T. Howard
A. F. H. Goetz
D. B. James
J. Z. Menard
J. M. Nervik
I. M. Ross
P. F. Sennewald
R. V. Sperry
J. W. Timko
R. L. Wagner
M. P. Wilson
Division 101 Supervision
All Members Division 102
Department 1024 Files
Central Files
Library